Learning Geometric Algebra by Modeling Motions of the Earth and Shadows of Gnomons to Predict Solar Azimuths and Altitudes

April 24, 2018

James Smith
nitac14b@yahoo.com
https://mx.linkedin.com/in/james-smith-1b195047

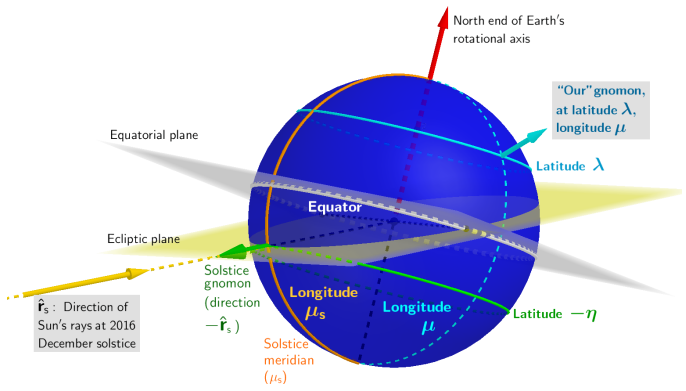

"Our first step in developing an expression for the orientation of "our" gnomon: Diagramming its location at the instant of the 2016 December solstice."

Abstract

Because the shortage of worked-out examples at introductory levels is an obstacle to widespread adoption of Geometric Algebra (GA), we use GA to calculate Solar azimuths and altitudes as a function of time via the heliocentric model. We begin by representing the Earth's motions in GA terms. Our representation incorporates an estimate of the time at which the Earth would have reached perihelion in 2017 if not affected by the Moon's gravity. Using the geometry of the December 2016 solstice as a starting

point, we then employ GA's capacities for handling rotations to determine the orientation of a gnomon at any given latitude and longitude during the period between the December solstices of 2016 and 2017. Subsequently, we derive equations for two angles: that between the Sun's rays and the gnomon's shaft, and that between the gnomon's shadow and the direction "north" as traced on the ground at the gnomon's location. To validate our equations, we convert those angles to Solar azimuths and altitudes for comparison with simulations made by the program Stellarium. As further validation, we analyze our equations algebraically to predict (for example) the precise timings and locations of sunrises, sunsets, and Solar zeniths on the solstices and equinoxes. We emphasize that the accuracy of the results is only to be expected, given the high accuracy of the heliocentric model itself, and that the relevance of this work is the efficiency with which that model can be implemented via GA for teaching at the introductory level. On that point, comments and debate are encouraged and welcome.

Contents

List of Figures

List of Tables

1 Introduction

Geometric Algebra (GA) holds promise as a means for formulating and solving problems in many different branches of mathematics and science. This document contributes to addressing one of the obstacles to GA's wider adoption: the shortage of instructional materials that use GA to solve non-trivial problems that are accessible to students who are in high school or the first year of university.

In this document, we'll use GA for calculations that are related to gnomons (Fig. 1) —astronomical instruments of a type that dates to antiquity. Many simple, interesting experiments that use it are described in detail on line (e.g. [2]), and can be performed by students to check predictions such as those which we will make here. We will see, too, that through use of simple geometric and trigonometric relations, inferences drawn from our gnomon equations can be transformed into predictions that we can check via free planetarium software such as Stellarium ([3]).

A key goal of this document is to make clear the relationship between the skill of modeling physical systems, and the nature and capabilities of the mathematical tools that are available to the modeler. The gnomon is a good example for teaching that relationship because it shows the benefits of "seeing" a system in terms of rotations—an operation to which GA is especially suited. Toward that end, our specific goals will be

1. To use GA to predict the following for any location on Earth, at any time between the December 2016 solstice and the December 2017 solstice:
   (a) the angle between the Sun's rays and the gnomon; and
   (b) the angle between local north and the gnomon's shadow.
2. To validate our model by comparing our predictions to results of simple gnomon observations, and to simulations made by the planetarium program Stellarium ([3]).

The same calculations may be done for other years using data available at [4].

This document begins by reviewing relevant information on Kepler orbits, the geometry of the Earth's orientation with respect to the plane of its orbit about the Sun, and GA. Based upon that review, we'll develop a model, then derive the necessary equations. We'll find that they are surprisingly amenable to analyses that let us test key predictions without needing to do numerical calculations. (Although we will of course do such calculations as well.)

Figure 1: Students using a gnomon at a school in India ([1]).

2 Review of Relevant Information about Kepler Orbits, Earth's orientation, and GA

"Our" gnomon.

To get the most out of this review, we'll want to keep the document's goals in mind. Let's state them again, but this time we'll refer to the gnomon for which we want to calculate angles, etc. as simply "our gnomon":

1. To use Geometric algebra to predict the following, at any time between the December 2016 solstice and the December 2017 solstice:
   (a) the angle between the Sun's rays and our gnomon; and
   (b) the angle between local north and our gnomon's shadow.
2. To validate our model by comparing our predictions to results of simple gnomon observations, and to simulations made by the planetarium program Stellarium ([3]).

Given our goals, a reasonable thing to look for during our review is some specific moment at which we can identify both of the following: the direction of the Sun's rays, and the direction in which our gnomon is pointing. Our goal would then be to find a way to use that information to calculate, via GA, those same directions for any other instant in time that might interest us.

2.1 The Gnomon and Its Uses

A gnomon is nothing more than a vertical stick, pole, or (in some cases) structure surrounded by a flat, horizontal surface of appropriate size (Fig. 2). Over the course of a year, the trajectory followed by the end of the gnomon's shadow changes systematically from one day to the next. Most notably, that trajectory is an almost-perfect east-west line on the days of the equinoxes ([2]). Typical experiments done with gnomons include tracing that trajectory for subsequent mathematical analysis. Younger students enjoy measuring the angle β between local north and the gnomon's shadow, and the angle α between the gnomon and a string stretched from the tip of the gnomon to the end of the shadow (Figs. 3 and 4).

Figs. 3 –5 and Table 1 show how to determine the Sun's azimuth and altitude from the angles α and β.

The shaft of the gnomon can be regarded as an extension of the line segment that runs from the center of the Earth to the gnomon's base.

Please note something that will be important in our development of a model: because the Earth's deviation from perfect sphericity is less than 0.3% ([5]), the shaft of the gnomon can be regraded as an extension of the line segment that runs from the center of the Earth to the gnomon's base.

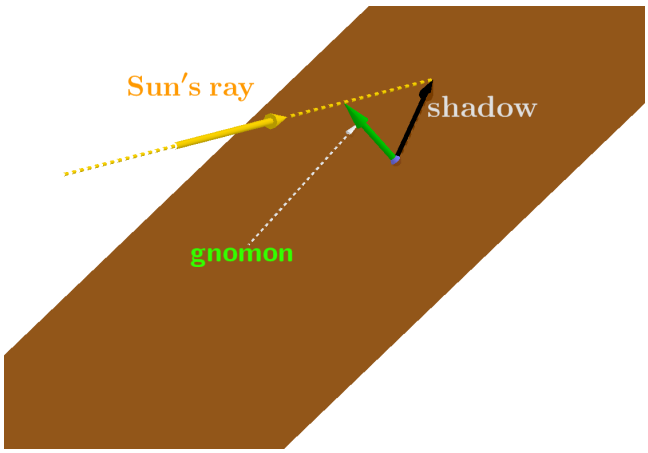

Figure 2: Schematic diagram of the Sun, the gnomon, and the gnomon's shadow on the flat, horizontal surface surrounding the gnomon.

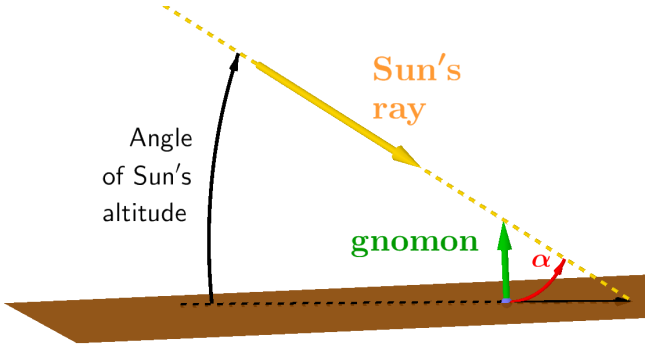

Figure 3: Showing the angle α between the Sun's rays and the shaft of the gnomon. The angle of the Sun's altitude (also called the angle of elevation) is the complement of α.

Table 1: Formulas for calculating azimuths according to the algebraic signs of $\sin\beta$ and $\cos\beta$. For example, if $\sin\beta < 0$ and $\cos\beta \geq 0$, then Azimuth $= 180^\circ + \arcsin|\sin\beta|$.

	$\underline{\sin\beta < 0}$	$\underline{\sin\beta \geq 0}$
$\cos\beta < 0$	$360^\circ - \arcsin\lvert\sin\beta\rvert$	$\arcsin\lvert\sin\beta\rvert$
$\cos\beta \geq 0$	$180^\circ + \arcsin\lvert\sin\beta\rvert$	$180^\circ - \arcsin\lvert\sin\beta\rvert$

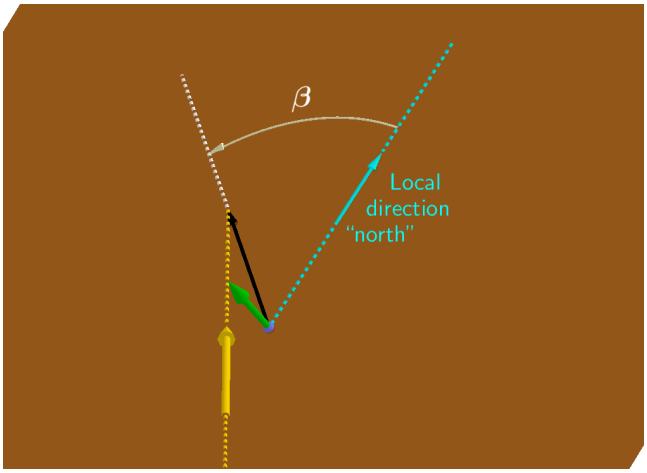

Figure 4: β is the angle of rotation from "Local North" (i.e., the direction "geographic north" as traced on the ground at the observer's location) and the gnomon's shadow. Later in this document, we will define the counterclockwise sense of β as positive.

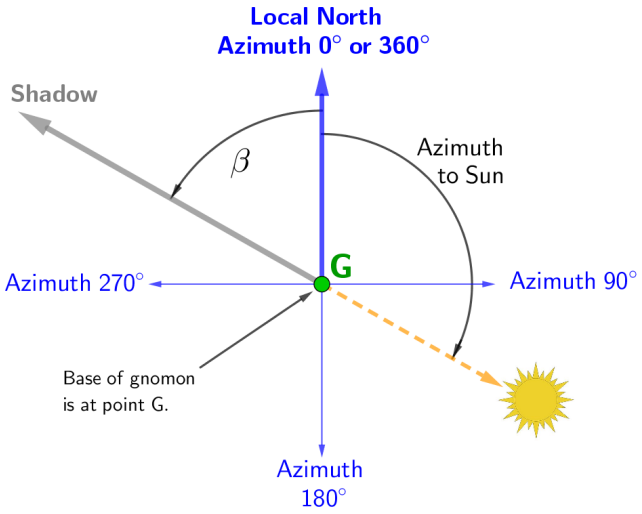

Figure 5: Geometrical bases for the formulas presented in Table 1 for determining the Sun's azimuth from $\sin\beta$ and $\cos\beta$. Diagram is a schematic of an aerial view of a plaza in which our gnomon is set. The Sun is in the part of the sky opposite the shadow. Angle β is positive counter-clockwise from local north, and the Sun's azimuth is positive clockwise from local north.

2.2 The Earth's Kepler Orbit, and the Geometry of Solstices and Equinoxes

2.2.1 The Earth's Kepler Orbit

Fig. 6 shows key elements that we will use later: the vector $\hat{\mathbf{r}}$ from the center of the Sun to the center of the Earth; the angles θ and ϕ; and the vector $\mathbf{a}$, from the center of the orbit through the center of the Sun, to the position of the Earth's center at perihelion.

Hestenes ([6], pp. 204-219) used GA to arrive at the well-known *Kepler equation* for planetary motion:

$$\frac{2\pi t}{T} = \phi - \epsilon \sin \phi. \tag{2.1}$$

where T is the planet's orbital period, t is the time elapsed since the planet was at its perihelion, and ϵ is the orbit's eccentricity. The angle ϕ is in radians.

For any given time t, the corresponding angle $\theta(t)$ is determined by first solving Eq. (2.1) for $\phi(t)$, after which the corresponding value of θ is found ([6], p. 219) via the relationship

$$\tan \frac{\theta}{2} = \left(\frac{1+\epsilon}{1-\epsilon} \right)^{1/2} \tan \frac{\phi}{2}, \tag{2.2}$$

from which

$$\theta = 2 \tan^{-1} \left[\left(\frac{1+\epsilon}{1-\epsilon} \right)^{1/2} \tan \frac{\phi}{2} \right]. \tag{2.3}$$

Ref. [7] notes that for works like the present, we must estimate what the timing and position of the Earth's perihelion would be if the Earth's orbit were a perfect Keplerian ellipse that is unperturbed by the gravity of other bodies, especially the Moon. Using a best-fit method, [7] estimated that the perihelion of 2017 occurred 12.93 days after the instant of the December 2016 solstice, and that that solstice therefore occurred at angle θ of 0.2301 rad before perihelion (Fig. 7).

Note that Fig. 7 shows the line connecting the positions of the Earth at the equinoxes as being perpendicular the line connecting the positions at the solstices. Actually, there is a very slight non-perpendicularity because the Earth's axis precesses by about $1/70^\circ$ per year. That precession also causes a twenty-minute difference between the lengths of the Tropical year (the time between successive December solstices) and the Sidereal year (the time needed for the Earth to complete one revolution of its orbit, as measured against a fixed frame of reference such as the stars). The effects of precession will require us to be careful to use the Tropical year of 365.242 days in our calculations instead of the Sidereal year of 365.256 days, but will otherwise be negligible for our purposes. Differences between various types of year are discussed further in [8] and [9].

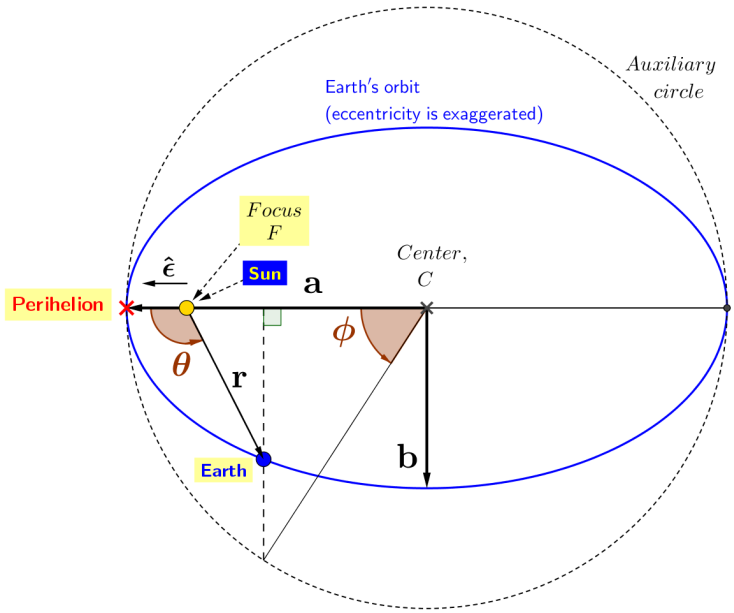

Figure 6: Schematic of the Earth's Kepler orbit, defining the elements ϕ, θ, ϵ, and $\hat{\mathbf{r}}$ used in this analysis. The plane of the Earth's orbit is known as the *ecliptic*. (Reproduced from [7].)

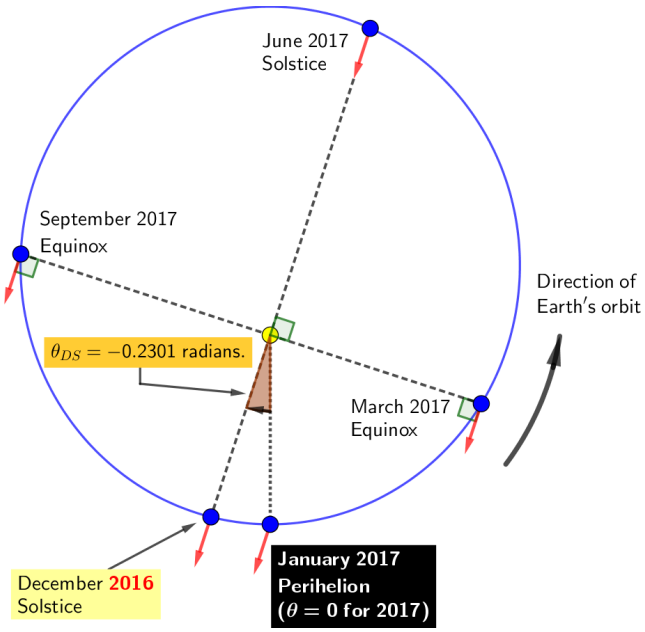

Figure 7: The position of the 2017 perihelion with respect to the December 2016 solstice. Red arrows show the direction in which the north end of the Earth's rotational axis points. The line connecting the positions of the Earth at the equinoxes is not perfectly perpendicular to the line connecting the positions at the solstices because the Earth's axis precesses by about $1/70^\circ$ per year. (Reproduced from [7].)

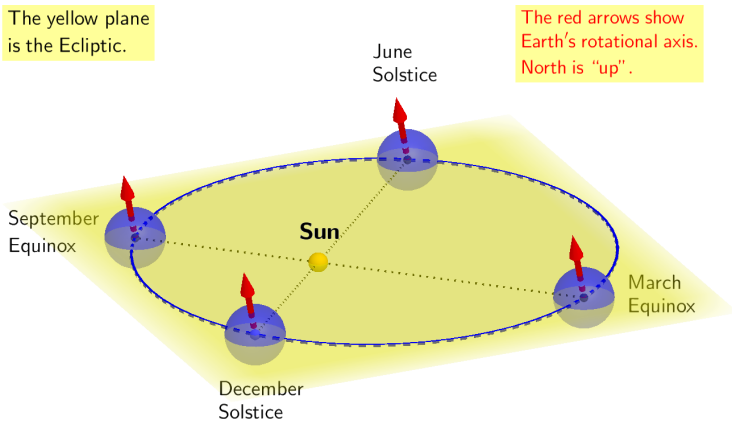

Figure 8: The relationship between the Sun, Earth, ecliptic, and the Earth's rotational axis. For our purposes, the orientation of the rotational axis is constant during a given year, and the line connecting the positions of the Earth at the equinoxes can be taken as perfectly perpendicular to the line connecting the positions at the solstices. (Reproduced from [7].)

2.2.2 Geometry of Solstices and Equinoxes

During a given year, we can treat the orientation of the Earth's equatorial plane as invariant.

As shown in Fig. 8, the Earth's rotational axis is inclined with respect to the plane of the Earth's orbit, or *ecliptic*. For our purposes the orientation of the rotational axis is constant during a given year (Section 2.2.1). Therefore, we can treat the orientation of the Earth's equatorial plane as invariant.

In the common language, the terms "equinox and "solstice" refer to days, but astronomers also use those terms to refer to precise instants as well. At the instant of an equinox, the Earth's axis of rotation lies within the plane that is perpendicular to the ecliptic and to the line connecting the centers of the Earth and Sun (Fig. 9). In contrast, at the instant of a solstice the axis lies within the plane that is perpendicular to the ecliptic, and which also contains the line that connects the centers of the Earth and Sun (Fig. 10).

Using ideas similar to those given in [10], we can identify the meridian of longitude that faces the Sun directly at any given instant. The specific instant that interests us is that of the December 2016 solstice.

2.2.3 Summary of our Review of the Earth's Orbit and the Geometry of Equinoxes and Solstices

Before we began to review this material, we had decided that as we went through each topic, we would look for some specific instant at which we could identify both of the following: (a) the direction of the Sun's rays, and (b) the direction in which our gnomon would be pointing.

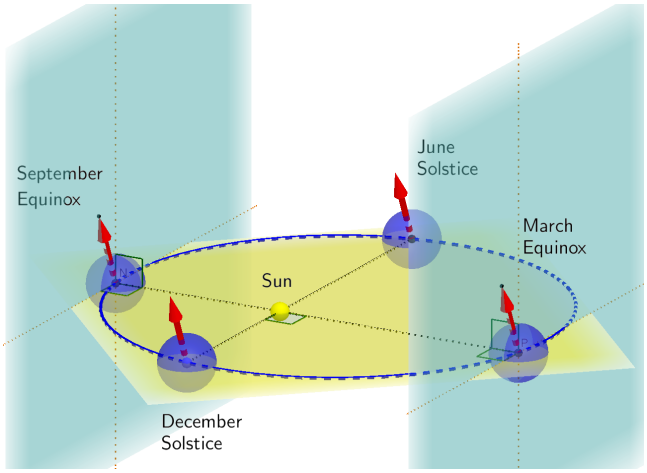

Figure 9: Geometry of the equinoxes: the Earth's axis of rotation lies within the plane that is perpendicular to the ecliptic and to the line connecting the centers of the Earth and Sun. (Reproduced from [7].)

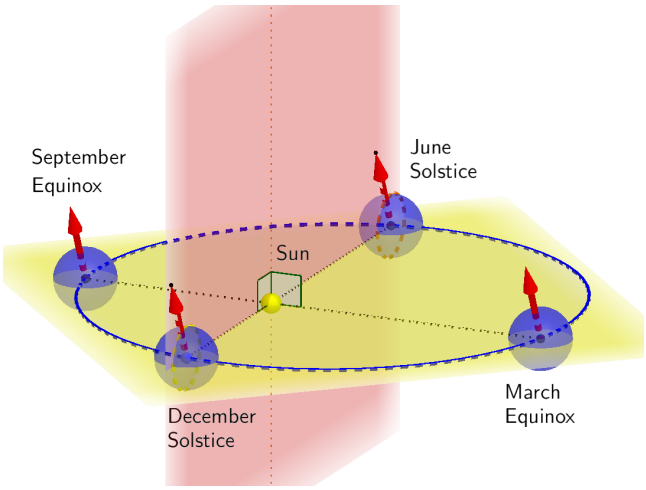

Figure 10: Geometry of the solstices: the Earth's axis of rotation lies within the plane that is perpendicular to the ecliptic, and which also contains the line that connects the centers of the Earth and Sun. (Reproduced from [7].)

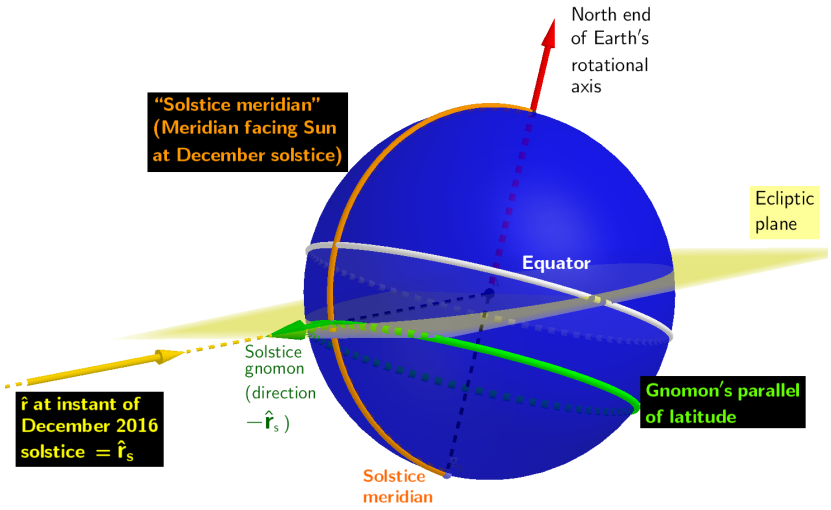

Figure 11: One of the goals of our review: finding a convenient instant at which a gnomon with a known location points in an identifiable direction. At the instant of the December 2016 solstice, a gnomon along the meridian that faces the Sun directly, and whose south latitude is equal to the angle of inclination of the Earth's rotational axis with respect to the ecliptic plane, will point in the direction $-\hat{\mathbf{r}}$.

The 2016 December solstice would seem to be a good choice. Although we don't know the orientation of our own gnomon at that instant, we can identify the location of a gnomon that points directly at the Sun at that instant: its latitude is equal to that of the Earth's inclination with respect to the ecliptic (Fig. 11), and its longitude is that of the meridian that faces the Sun directly. From that information, and the latitude and longitude of our own location, we should be able to determine the orientation of our gnomon at the instant of the 2016 December solstice.

We should also note that for our purposes, the Sun's rays that reach the Earth are parallel to $\hat{\mathbf{r}}$.

For our purposes, the Sun's rays that reach the Earth are parallel to $\hat{\mathbf{r}}$.

2.3 Review of GA

At the end of the previous section (2.2.3), we identified a combination of specific gnomon location and instant in time with respect to which we should be able to express the orientation of our own gnomon at any other instant t that might interest us. Of course, we will also be able to calculate the vector $\hat{\mathbf{r}}$ for any instant t via Eqs. (2.1) and (2.3). Now, we'll review what we've learned about GA so that we may learn how do the above via rotations, if practical.

2.3.1 Some General Comments on GA

As both a math tutor and a self-taught student, I am all too aware of the confusion that students experience when trying to form an accurate mental model of that which a classroom teacher or the author of a textbook is striving to communicate through a combination of words, symbols, and diagrams. I hope that the following observations might help, although they are not intended to be either rigorous or complete.

A sometimes-helpful recognition is that GA, as it applies to problems like the gnomon, is an attempt to capture geometric aspects of 3-D reality. The mathematicians who developed GA found that they could express that reality through concepts—of their own invention—which came to be known as vectors, bivectors, and trivectors, and through carefully-defined mathematical operations that are termed "products" of various sorts.

Of course this characterization of GA is vague, but the important points are that GA is a human invention, and that the choices of which concepts and operations were to be used in the attempt to formulate and solve geometrical problems was made by human beings. Those same human beings defined the properties of the concepts; for example, they decided that any two vectors of identical length, direction, and orientation are equal, regardless of where they are located in space. (Or perhaps to be more correct, "regardless of where their endpoints are located in space".) The originators of the concept of vectors did not include "position" among the characteristics of vectors for a very simple reason: there was no need to do so, and they saw no benefit in doing so.

Similar comments apply to bivectors: their only characteristics are magnitude ("area", in 3-D geometry), orientation, and sense (algebraic sign). Developers of GA were able to accomplish their goals without including shape and location among bivectors' characteristics.

To accomplish our own, gnomon-related goals via GA, we need to express the ecliptic plane in terms of a specific GA bivector (one to which the plane is parallel). We also need to express the relation between that bivector and the one that is used for the equatorial plane, and we need to express each of these bivectors in terms of the basis bivectors of whatever reference system we might find convenient. Rather than go into those important skills in detail here, we'll see how to put them into practice when we develop our gnomon model, and when we derive formulas for calculating the angles α and β. Additional examples can be found in [11] and [12].

One final note before we review the relevant GA information: in this document, there are times when we will use the symbol for a given bivector (e.g., $\mathbf{Q}$) to represent both the bivector itself (which is a GA object) and the plane to which that bivector is parallel. Where the meaning of the symbol is not made clear by context, we'll state, explicitly, which meaning is intended.

In somewhat the same vein, we should mention that we may talk about rotating a physical plane (such as the plane that contains the meridian of longitude on which a gnomon stands) in terms of rotating the bivector that represents it. Said meridian rotates with the Earth, so in that sense the meridian does rotate. However, when we are using the term "plane" in its strict Euclidean sense, a plane is a distinct set of points. Thus, the rotation of a plane produces a different plane, not the same plane in a different orientation. Similar comments apply to bivectors. Thus. as a the meridian rotates with the Earth, it goes into and out of alignment with a succession of bivectors.

To put that differently, let's use the symbol $\hat{\mathbf{M}}$ to denote the bivector that's parallel to the plane that contains a certain meridian. We see immediately that the bivector that's aligned with the plane at time t_1 may be different from that with which the meridian plane is aligned at some other time t_2. Therefore, "the" bivector with which the meridian is aligned is a function of time. We'll write that function as $\hat{\mathbf{M}}(t)$. Having done so, we recognize that although $\hat{\mathbf{M}}(t)$ is a *set of* bivectors, each $\hat{\mathbf{M}}(\tau)$ for any specific value τ of the time t is a *specific, individual* bivector.

2.3.2 Rotations and their Representations in GA

Let's recall that our purpose in this document is not only to calculate the angles α and β, etc., but also to learn how to employ GA effectively for the formulation and solution of certain types of problems. We expect, reasonably, that the gnomon problem will be a good one for learning how to use GA for expressing rotations, and also for determining angles between vectors. Refs. [11] and [12] treat those topics in detail, but we will present only the most-relevant and -important observations here.

Rotation of a vector by a bivector angle When describing an angle of rotation in GA, we are often well advised—for sake of clarity—to write it as the product of the angle's scalar measure (in radians) and the bivector of the plane of rotation. Following that practice, we would say that the rotation of a vector $\mathbf{w}$ through the angle γ (measured in radians) with respect to a plane that is parallel to the unit bivector $\hat{\mathbf{Q}}$, is the rotation of $\mathbf{w}$ through the *bivector angle* $\hat{\mathbf{N}}\gamma$. (For example, see Fig. 12.) References [6] (pp. 280-286) and [13] (pp. 89-91) derive and explain the following formula for finding the new vector, $\mathbf{w'}$, that results from that rotation :

$$\mathbf{w}' = \underbrace{\left[e^{-\hat{\mathbf{N}}\gamma/2}\right][\mathbf{w}]\left[e^{\hat{\mathbf{N}}\gamma/2}\right]}_{\text{Notation: } \mathsf{R}_{\hat{\mathbf{N}}\gamma}(\mathbf{w})}. \tag{2.4}$$

Notation: $\mathsf{R}_{\hat{\mathbf{N}}\gamma}(\mathbf{w})$ is the rotation of the vector $\mathbf{w}$ by the bivector angle $\hat{\mathbf{N}}\gamma$.

For our convenience later in this document, we will follow Reference [13] (p. 89) in saying that the factor $e^{-\hat{\mathbf{N}}\gamma/2}$ *represents* the rotation $\mathsf{R}_{\hat{\mathbf{N}}\gamma}$. That factor

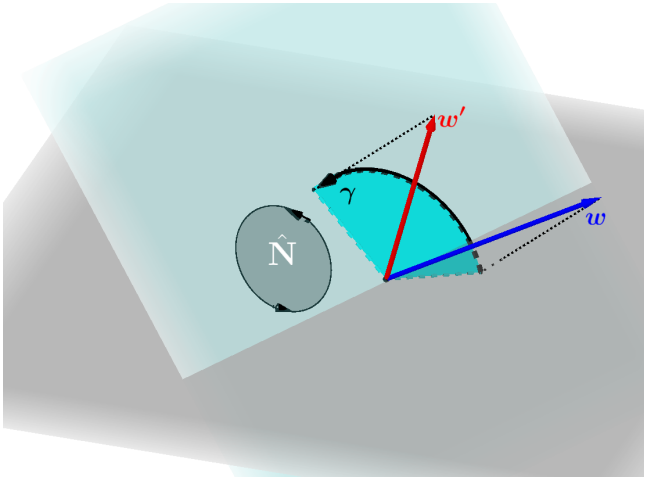

Figure 12: Rotation of the vector $\mathbf{w}$ through the bivector angle $\hat{\mathbf{N}}\gamma$, to produce the vector $\mathbf{w}'$.

The *representation* of a rotation.

is a quaternion, but in GA terms it is a multivector. We can see that from the following identity, which holds for any unit bivector $\hat{\mathbf{B}}$ and any angle ξ (measured in radians):

$$exp\left(\hat{\mathbf{B}}\xi\right) \equiv \cos\xi + \hat{\mathbf{B}}\sin\xi.$$

Thus,

$$e^{-\hat{\mathbf{N}}\gamma/2} = \cos\tfrac{\gamma}{2} - \hat{\mathbf{N}}\sin\tfrac{\gamma}{2}. \tag{2.5}$$

In our choice of symbols for basis vectors and bivectors, we´re following [13], p. 82.

In this document, we'll restrict our treatment of rotations to three-dimensional Geometric Algebra ($\mathbb{G}^3$). In that algebra, and using a right-handed reference system with orthonormal basis vectors $\hat{\mathbf{a}}$, $\hat{\mathbf{b}}$, and $\hat{\mathbf{c}}$, we may express the unit bivector $\hat{\mathbf{N}}$ as a linear combination of the basis bivectors $\hat{\mathbf{a}}\hat{\mathbf{b}}$, $\hat{\mathbf{b}}\hat{\mathbf{c}}$, and $\hat{\mathbf{a}}\hat{\mathbf{c}}$:

$$\hat{\mathbf{N}} = \hat{\mathbf{a}}\hat{\mathbf{b}}n_{ab} + \hat{\mathbf{b}}\hat{\mathbf{c}}n_{bc} + \hat{\mathbf{a}}\hat{\mathbf{c}}n_{ac},$$

in which n_{ab}, n_{bc}, and n_{ac} are scalars, and $n_{ab}^2 + n_{bc}^2 + n_{ac}^2 = 1$.

If we now write $\mathbf{w}$ as $\mathbf{w} = \hat{\mathbf{a}}w_a + \hat{\mathbf{b}}w_b + \hat{\mathbf{c}}w_c$, Eq. (2.4) becomes

$$\begin{aligned}\mathbf{w}' &= \left[\cos\tfrac{\gamma}{2} - \hat{\mathbf{N}}\sin\tfrac{\gamma}{2}\right][\mathbf{w}]\left[\cos\tfrac{\gamma}{2} + \hat{\mathbf{N}}\sin\tfrac{\gamma}{2}\right] \\ &= \left[\cos\tfrac{\gamma}{2} - \left(\hat{\mathbf{a}}\hat{\mathbf{b}}q_c + \hat{\mathbf{b}}\hat{\mathbf{c}}q_a - \hat{\mathbf{a}}\hat{\mathbf{c}}q_b\right)\sin\tfrac{\gamma}{2}\right]\left[\hat{\mathbf{a}}w_a + \hat{\mathbf{b}}w_b + \hat{\mathbf{c}}w_c\right]\left[\cos\tfrac{\gamma}{2} + \left(\hat{\mathbf{a}}\hat{\mathbf{b}}q_c + \hat{\mathbf{b}}\hat{\mathbf{c}}q_a - \hat{\mathbf{a}}\hat{\mathbf{c}}q_b\right)\sin\tfrac{\gamma}{2}\right]. \end{aligned} \tag{2.6}$$

Expanding the right-hand side of that result, we'd obtain 48 (!) terms, some of which would simplify to scalar multiples of $\hat{\mathbf{a}}$, $\hat{\mathbf{b}}$, and $\hat{\mathbf{c}}$, and others of which will simplify to scalar multiples of the trivector $\hat{\mathbf{a}}\hat{\mathbf{b}}\hat{\mathbf{c}}$. The latter terms would cancel, leaving an expression for $\mathbf{w}'$ in terms of $\hat{\mathbf{a}}$, $\hat{\mathbf{b}}$, and $\hat{\mathbf{c}}$.

Now, we define four scalar variables:

- $f_o = \cos\dfrac{\gamma}{2}$;
- $f_{ab} = n_{ab}\sin\dfrac{\gamma}{2}$;
- $f_{bc} = n_{bc}\sin\dfrac{\gamma}{2}$; and
- $f_{ac} = n_{ac}\sin\dfrac{\gamma}{2}$.

Using these variables, Eq. (2.6) becomes

$$\mathbf{w}' = \left[f_o - \left(\hat{\mathbf{a}}\hat{\mathbf{b}}f_{ab} + \hat{\mathbf{b}}\hat{\mathbf{c}}f_{bc} + \hat{\mathbf{a}}\hat{\mathbf{c}}f_{ac}\right)\right]\left[\hat{\mathbf{a}}w_a + \hat{\mathbf{b}}w_b + \hat{\mathbf{c}}w_c\right]\left[f_o + \left(\hat{\mathbf{a}}\hat{\mathbf{b}}f_{ab} + \hat{\mathbf{b}}\hat{\mathbf{c}}f_{bc} + \hat{\mathbf{a}}\hat{\mathbf{c}}f_{ac}\right)\right].$$

After expanding and simplifying the right-hand side, we obtain

$$\begin{aligned}\mathbf{w}' = {} & \hat{\mathbf{a}}\left[w_a\left(f_o^2 - f_{ab}^2 + f_{bc}^2 - f_{ac}^2\right) + w_b\left(-2f_of_{ab} - 2f_{bc}f_{ac}\right) + w_c\left(-2f_of_{ac} + 2f_{ab}f_{bc}\right)\right] \\ & + \hat{\mathbf{b}}\left[w_a\left(2f_of_{ab} - 2f_{bc}f_{ac}\right) + w_b\left(f_o^2 - f_{ab}^2 - f_{bc}^2 + f_{ac}^2\right) + w_c\left(-2f_of_{bc} - 2f_{ab}f_{ac}\right)\right] \\ & + \hat{\mathbf{c}}\left[w_a\left(2f_of_{ac} + 2f_{ab}f_{bc}\right) + w_b\left(2f_of_{bc} - 2f_{ab}f_{ac}\right) + w_c\left(f_o^2 + f_{ab}^2 - f_{bc}^2 - f_{ac}^2\right)\right].\end{aligned} \tag{2.7}$$

Note that in terms of our four scalar variables f_o, f_{ab}, f_{bc}, and f_{ac}, the representation $\left(e^{-\hat{\mathbf{N}}\gamma/2}\right)$ of the rotation is

$$e^{-\hat{\mathbf{N}}\gamma/2} = f_o - \left(\hat{\mathbf{a}}\hat{\mathbf{b}}f_{ab} + \hat{\mathbf{b}}\hat{\mathbf{c}}f_{bc} + \hat{\mathbf{a}}\hat{\mathbf{c}}f_{ac}\right). \tag{2.8}$$

Because of the convenience with which Eq. (2.7) can be implemented, the remainder of this document will express the representations of various rotations of interest in the form of Eq. (2.8).

Rotation of a bivector Fig. 13 illustrates the rotation of a bivector $\mathbf{P}$ by the bivector angle $\hat{\mathbf{N}}\gamma$ to give a new bivector, $\mathbf{H}$. In his Theorem 7.5, Macdonald ([13], p. 125) states that if a blade $\mathbf{P}$ is rotated by the bivector angle $\hat{\mathbf{N}}\gamma$, the result will be the blade

$$\mathsf{R}_{\hat{\mathbf{N}}\gamma}(\mathbf{P}) = \left[e^{-\hat{\mathbf{N}}\gamma/2}\right][\mathbf{P}]\left[e^{\hat{\mathbf{N}}\gamma/2}\right]. \tag{2.9}$$

To express the result as a linear combination of the unit bivectors $\hat{\mathbf{a}}\hat{\mathbf{b}}$, $\hat{\mathbf{b}}\hat{\mathbf{c}}$, and $\hat{\mathbf{a}}\hat{\mathbf{c}}$, we begin by writing the unit bivector $\hat{\mathbf{N}}$ as $\hat{\mathbf{N}} = \hat{\mathbf{a}}\hat{\mathbf{b}}n_{ab} + \hat{\mathbf{b}}\hat{\mathbf{c}}n_{bc} + \hat{\mathbf{a}}\hat{\mathbf{c}}n_{ac}$, so that we may write the representation of the rotation in exactly the same way as we did for the rotation of a vector:

$$e^{-\hat{\mathbf{N}}\gamma/2} = f_o - \left(\hat{\mathbf{a}}\hat{\mathbf{b}}f_{ab} + \hat{\mathbf{b}}\hat{\mathbf{c}}f_{bc} + \hat{\mathbf{a}}\hat{\mathbf{c}}f_{ac}\right),$$

with $f_o = \cos\dfrac{\gamma}{2}$; $f_{ab} = n_{ab}\sin\dfrac{\gamma}{2}$; $f_{bc} = n_{bc}\sin\dfrac{\gamma}{2}$; $f_{ac} = n_{ac}\sin\dfrac{\gamma}{2}$.

Next, we write $\mathbf{P}$ as $\mathbf{P} = \hat{\mathbf{a}}\hat{\mathbf{b}}p_{ab} + \hat{\mathbf{b}}\hat{\mathbf{c}}p_{bc} + \hat{\mathbf{a}}\hat{\mathbf{c}}p_{ac}$. Making these substitutions in Eq. (2.9), then expanding and simplifying, we obtain

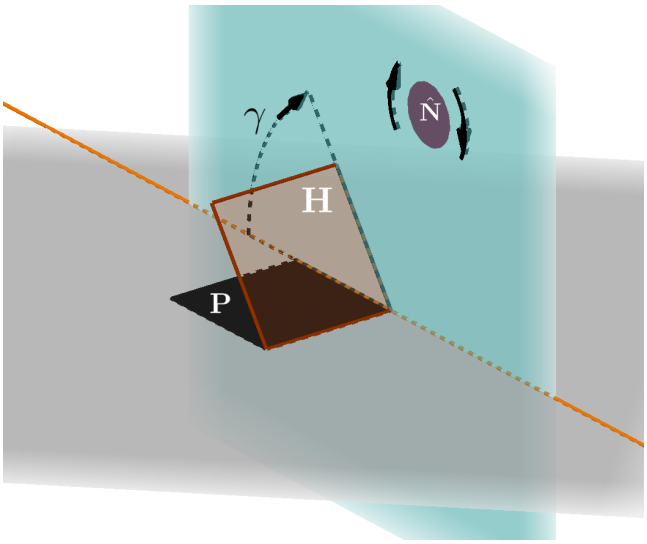

Figure 13: Rotation of bivector $\mathbf{P}$ by the bivector angle $\hat{\mathbf{N}}\gamma$ to give the bivector $\mathbf{H}$.

$$
\begin{aligned}
\mathsf{R}_{\hat{\mathbf{N}}\gamma}(\mathbf{P}) = \hat{\mathbf{a}}\hat{\mathbf{b}} \{ & p_{ab}\left(1 - 2f_{bc}^2 - 2f_{ac}^2\right) \\
& +2\left[f_{ab}\left(f_{bc}p_{bc} + f_{ac}p_{ac}\right) + f_o\left(f_{ac}p_{bc} - f_{bc}p_{ac}\right)\right]\} \\
+ \hat{\mathbf{b}}\hat{\mathbf{c}} \{ & p_{bc}\left(1 - 2f_{ab}^2 - 2f_{ac}^2\right) \\
& +2\left[f_{bc}\left(f_{ab}p_{ab} + f_{ac}p_{ac}\right) + f_o\left(f_{ab}p_{ac} - f_{ac}p_{ab}\right)\right]\} \\
+ \hat{\mathbf{a}}\hat{\mathbf{c}} \{ & p_{ac}\left(1 - 2f_{ab}^2 - 2f_{bc}^2\right) \\
& +2\left[f_{ac}\left(f_{ab}p_{ab} + f_{bc}p_{bc}\right) + f_o\left(f_{bc}p_{ab} - f_{ab}p_{bc}\right)\right]\}.
\end{aligned}
\tag{2.10}
$$

2.3.3 Angles Between Projected Vectors

Ref. [12] treats this topics in detail, noting that the direction that we have been calling "local north" is the perpendicular projection of the Earth's rotational axis upon a plane that is tangent to the Earth's surface (assumed perfectly spherical) at the gnomon's location (Figs. 14 and 15).

Another observation in [12] is that the gnomon's shadow is the the projection of $\hat{\mathbf{r}}$ upon that same plane. Thus, our angle β is the angle between those two projections. Ref. [12] considered precisely that sort of problem in GA terms: the angle between the projections of two vectors, $\mathbf{u}$ and $\mathbf{v}$, upon a unit bivector $\hat{\mathbf{P}}$ whose dual is $\hat{\mathbf{e}}$ (Fig. 16). Writing these elements as

- $\mathbf{u} = \hat{\mathbf{a}}u_a + \hat{\mathbf{b}}u_b + \hat{\mathbf{c}}u_c$,

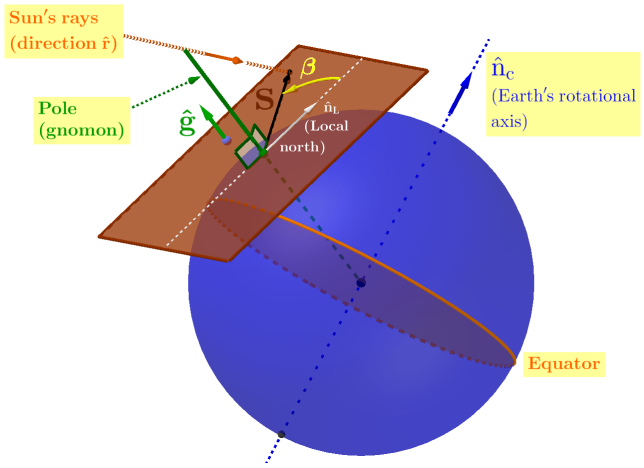

Figure 14: Reproduced from [12]. The flat, horizontal surface surrounding the gnomon is a plane tangent to the Earth (assumed spherical) at the point at which our gnomon is embedded .

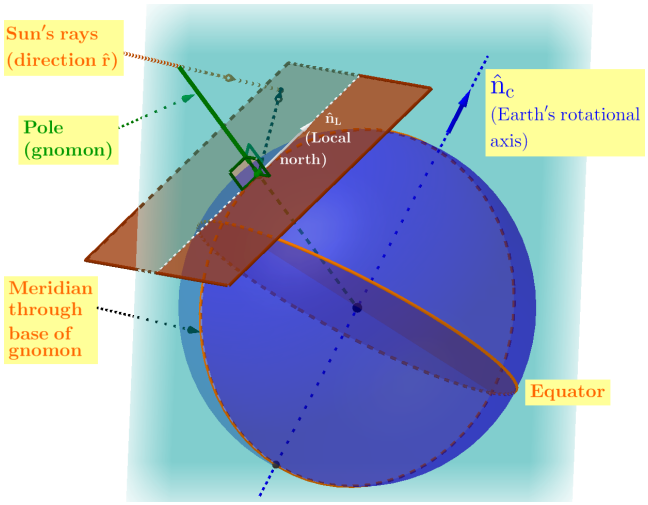

Figure 15: Reproduced from [12]. Note that the plane that contains the Earth's rotational axis and the meridian on which the gnomon is located cuts the tangent plane along the direction that we have been calling "local north". Therefore, the direction "local north" is the perpendicular projection of the direction of the Earth's rotational axis (labeled here as $\hat{\mathbf{n}}_c$) upon the flat, horizontal surface on which our gnomon stands.

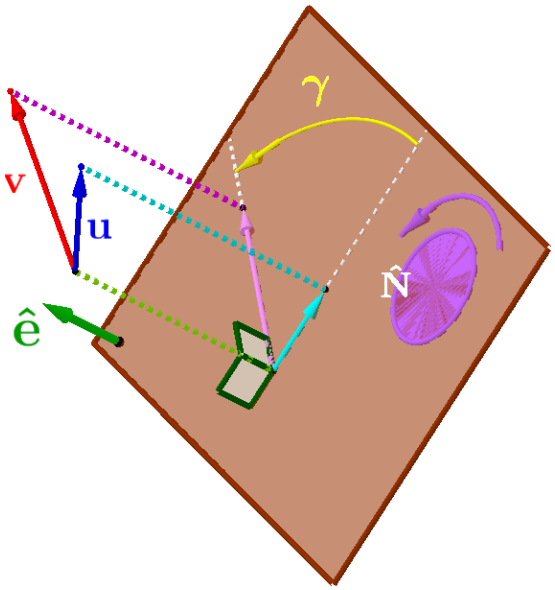

Figure 16: The problem treated in GA terms by [12]: the angle between the projections of two vectors, $\mathbf{u}$ and $\mathbf{v}$, upon a unit bivector $\hat{\mathbf{N}}$ whose dual is $\hat{\mathbf{e}}$.

- $\mathbf{v} = \hat{\mathbf{a}} v_a + \hat{\mathbf{b}} v_b + \hat{\mathbf{c}} v_c$,
- $\mathbf{e} = \hat{\mathbf{a}} e_a + \hat{\mathbf{b}} e_b + \hat{\mathbf{c}} e_c$, and
- $\hat{\mathbf{N}} = \hat{\mathbf{a}}\hat{\mathbf{b}} n_{ab} + \hat{\mathbf{b}}\hat{\mathbf{c}} n_{bc} + \hat{\mathbf{a}}\hat{\mathbf{c}} n_{ac} \left(= \hat{\mathbf{a}}\hat{\mathbf{b}} e_c + \hat{\mathbf{b}}\hat{\mathbf{c}} e_a - \hat{\mathbf{a}}\hat{\mathbf{c}} e_b \right)$,

[12] found that

$$\sin\gamma = \frac{(u_a v_b - u_b v_a)\, n_{ab} + (u_b v_c - u_c v_b)\, n_{bc} + (u_a v_c - u_c v_a)\, n_{ac}}{\|\mathbf{u}\cdot\hat{\mathbf{N}}\|\|\mathbf{v}\cdot\hat{\mathbf{N}}\|},$$

$$= \frac{(u_a v_b - u_b v_a)\, e_c + (u_b v_c - u_c v_b)\, e_a - (u_a v_c - u_c v_a)\, e_b}{\|\mathbf{u}\cdot\hat{\mathbf{N}}\|\|\mathbf{v}\cdot\hat{\mathbf{N}}\|}, \tag{2.11}$$

where $\|\mathbf{u}\cdot\hat{\mathbf{N}}\|$ and $\|\mathbf{v}\cdot\hat{\mathbf{N}}\|$ are the square roots of the expressions

$$\begin{aligned}\|\mathbf{u}\cdot\hat{\mathbf{N}}\|^2 = {} & u_a^2\left(1-e_a^2\right) + u_b^2\left(1-e_b^2\right) + u_c^2\left(1-e_c^2\right) \\ & - 2u_a u_b e_a e_b - 2u_b u_c e_b e_c - 2u_a u_c e_a e_c\ ,\end{aligned} \tag{2.12a}$$

and

$$\begin{aligned}\|\mathbf{v}\cdot\hat{\mathbf{N}}\|^2 = {} & v_a^2\left(1-e_a^2\right) + v_b^2\left(1-e_b^2\right) + v_c^2\left(1-e_c^2\right) \\ & - 2v_a v_b e_a e_b - 2v_b v_c e_b e_c - 2v_a v_c e_a e_c\ .\end{aligned} \tag{2.12b}$$

Those expressions reduce to

$$\begin{aligned}\|\mathbf{u}\cdot\hat{\mathbf{N}}\|^2 &= u^2-(\mathbf{u}\cdot\hat{\mathbf{e}})^2 \\ &= u_a^2+u_b^2+u_c^2-\left(u_ae_a+u_be_b+u_ce_c\right)^2\ ,\end{aligned} \tag{2.13a}$$

and

$$\begin{aligned}\|\mathbf{v}\cdot\hat{\mathbf{N}}\|^2 &= v^2-(\mathbf{v}\cdot\hat{\mathbf{e}})^2 \\ &= v_a^2+v_b^2+v_c^2-\left(v_ae_a+v_be_b+v_ce_c\right)^2\ .\end{aligned} \tag{2.13b}$$

Ref. [12] also found that

$$\cos\gamma=\frac{\langle\left(\mathbf{u}\cdot\hat{\mathbf{N}}\right)\left(\mathbf{v}\cdot\hat{\mathbf{N}}\right)\rangle_0}{\|\mathbf{u}\cdot\hat{\mathbf{N}}\|\|\mathbf{v}\cdot\hat{\mathbf{N}}\|}, \tag{2.14}$$

where

$$\begin{aligned}\langle\left(\mathbf{u}\cdot\hat{\mathbf{N}}\right)\left(\mathbf{v}\cdot\hat{\mathbf{N}}\right)\rangle_0 &= u_av_a\left(1-n_{bc}^2\right)+u_bv_b\left(1-n_{ac}^2\right) \\ &\quad+u_cv_c\left(1-n_{ab}^2\right)-\left(u_av_c+u_cv_a\right)n_{ab}n_{bc} \\ &\quad+\left(u_bv_c+u_cv_b\right)n_{ab}n_{ac}+\left(u_av_b+u_bv_a\right)n_{bc}n_{ac},\end{aligned}$$

$$\begin{aligned}&= u_av_a\left(1-e_a^2\right)+u_bv_b\left(1-e_b^2\right) \\ &\quad+u_cv_c\left(1-e_c^2\right)-\left(u_av_c+u_cv_a\right)e_ae_c \\ &\quad-\left(u_bv_c+u_cv_b\right)e_be_c-\left(u_av_b+u_bv_a\right)e_ae_b.\end{aligned} \tag{2.15}$$

For our gnomon problem, the relevance of the above equations is that (1) the unit vector that points from the center of the Earth to the tip of the gnomon is also the dual of the bivector that is parallel to the plane on which the gnomon is erected, and (2) the direction of the Sun's rays is $\hat{\mathbf{r}}$ (Section 2.2.3).

2.4 Observations on the Background

One purpose of our review was to find a specific instant at which we could identify both of the following: the direction of the Sun's rays, and the direction in which our gnomon is pointing. Fig. 11, showing the geometry of the 2016 December solstice, seems to provide a good starting point. We can now attempt to use that information to calculate, via GA, the direction of the Sun's rays and our own gnomon at any other instant.

Below, we'll add the subscript L to $\hat{\mathbf{g}}$ to denote the orientation of "our" gnomon, and have used $\hat{\mathbf{g}}_L(t)$ instead of simply $\hat{\mathbf{g}}_L$ in recognition of the fact that the orientation of the gnomon on a rotating Earth is a function of time.

To express the following additional observations more conveniently, we'll denote the unit vector of the direction from the Earth's center to the tip of our

gnomon as $\hat{\mathbf{g}}_L(t)$, where t is the time elapsed since the Earth was at perihelion. We'll also note that $\hat{\mathbf{r}}$, too, is a function of t, and write it as $\hat{\mathbf{r}}(t)$. Similarly, α is $\alpha(t)$, and β is $\beta(t)$. Here, then, are the observations that might be most useful:

1. The key elements in our problem appear to be the direction of the Sun's rays; the ecliptic plane; the Earth's axis of rotation; and the Earth's equatorial plane.

2. The ecliptic plane, equatorial plane, and direction of the Earth's rotational axis can all be taken as invariant.

3. So that we may use the Kepler equation and its various transformations, we are well advised to define the time t as Kepler did. That is, $t = 0$ when the Earth is at perihelion.

4. The direction of the Sun's rays can be taken as $\hat{\mathbf{r}}(t)$.

5. From Figs. 3 and 11, we can deduce that $\cos\alpha(t) = \hat{\mathbf{r}}(t) \cdot [-\hat{\mathbf{g}}_L(t)]$.

6. The direction "Local north" is the projection of the Earth's rotational axis upon the plane that is tangent to the Earth at the point at which our gnomon is fixed. Because of the Earth's rotation, local north is a function of t.

7. The gnomon's shadow is the projection of $\hat{\mathbf{r}}(t)$ upon that same plane.

8. To find the angle $\beta(t)$, given $\hat{\mathbf{r}}(t)$ and $\hat{\mathbf{g}}_L(t)$, we can use Eqs. (2.11) and (2.14).

9. To find $\hat{\mathbf{r}}(t)$ at any given time, we can use Eqs. (2.1) and (2.2) .

Hence, we now have all we need for deriving formulas expressing angles α and β for our gnomon at any time, if we can express the orientation of the gnomon itself as a function of time.

3 Detailed Formulation of Model in GA Terms

3.1 A Still-Unresolved Detail: How to Express $\hat{\mathbf{g}}_L(t)$: The Orientation of Our Gnomon as a Function of Time

One of the purposes of this document is to show one way in which we might puzzle through a problem like the gnomon, to arrive at a workable model and solution strategy. Therefore, rather than just present a formula for $\hat{\mathbf{g}}_L(t)$, we'll struggle with the problem a bit.

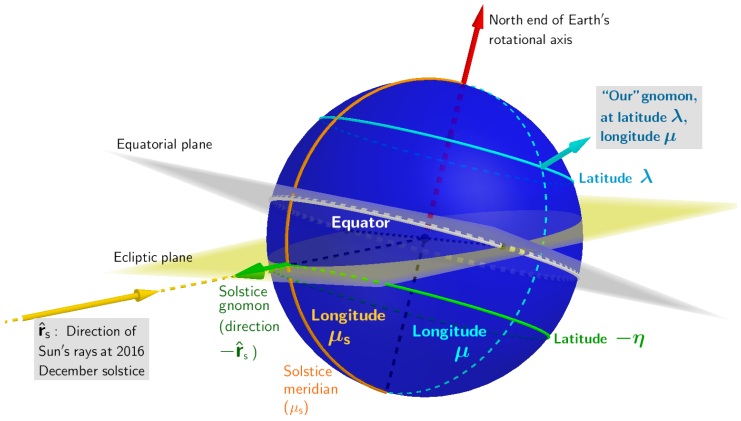

Figure 17: Our first step in developing an expression for the orientation of "our" gnomon at any time: making a diagram of its location and that of the solstice gnomon, in terms of their respective latitudes and longitudes, at the instant of the 2016 December solstice (t_s). The solstice gnomon is that which points directly at the Sun at that instant; thus, its orientation is $-\hat{\mathbf{r}}_s$.

3.1.1 Finding an Idea

At this moment, our question is, "What do we want?" The answer is, "An expression for $\hat{\mathbf{g}}_L(t)$."

So: what things did we note during our review, that might be useful? Here are three possibilities:

- Via GA, we can formulate, readily, rotations about a given axis or by a given bivector angle.
- The Earth rotates about its axis at a constant scalar angular velocity ω.
- We identified Fig. 11 as a promising starting-point for our present task.

An additional consideration might be that we should express the location of "our" gnomon via its latitude λ and its longitude μ.

Thinking through the above observations. we might draft something like Fig. 17, and conceive the follow overall plan:

1. First, we'll derive an expression for the orientation of "our" gnomon at the instant of the 2016 December solstice. We'll denote that instant by t_s. Thus, the vector that gives the orientation of our gnomon at that instant is $\hat{\mathbf{g}}(t_s)$.
2. To find an expression for the orientation of our gnomon at any other time t, we'll rotate $\hat{\mathbf{g}}(t_s)$ about the Earth's axis via GA.

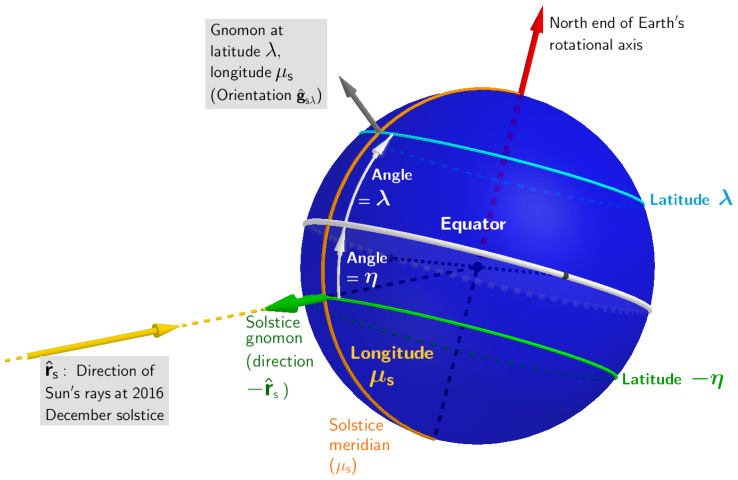

Figure 18: The second step in developing an expression for the orientation of our gnomon at any time: moving the solstice gnomon along the solstice meridian to the latitude (λ) of our gnomon. The vector of the gnomon in that position is $\hat{\mathbf{g}}_{s\lambda}$.

We should make a note to ourselves here, reminding us that we'll want to follow the usual convention of expressing northern latitudes as positive angles, and southern latitudes as negative ones.

Now, let's flesh out that plan a bit. At this stage, we may alternate between thinking in terms of "moving gnomons around on the globe" in Fig. 17, and rotating the corresponding vectors. So: how can we identify $\hat{\mathbf{g}}(t_s)$? One way is to recognize that we could do so by moving the solstice gnomon along meridians of longitude and parallels of longitude to the position of our gnomon. Thus, we would first slide the solstice gnomon along the solstice meridian, to the latitude (λ) of our gnomon (Fig. 18). In GA terms, that movement is the rotation of the vector $-\hat{\mathbf{r}}_s$ through the scalar angle $\lambda - (-\eta)$, $= \lambda + \eta$. We'll call the resulting vector $\hat{\mathbf{g}}_{s\lambda}$, and identify the bivector for that rotation later.

Another note to ourselves: we'll follow the usual convention of expressing eastern longitudes as positive angles, and western longitudes as negative ones.

Having "moved the solstice gnomon to our latitude", and called the result $\hat{\mathbf{g}}_{s\lambda}$, we'll now slide $\hat{\mathbf{g}}_{s\lambda}$ along our latitude until it stands on our meridian of longitude, μ (Fig. 19). In GA terms, that movement is a rotation by the scalar angle $\mu - \mu_s$ about the Earth's axis. The result will be the vector that we called $\hat{\mathbf{g}}(t_s)$: the orientation of our gnomon at the instant of the 2016 December solstice.

Now, to find the orientation of our gnomon at any other instant, t, we just rotate $\hat{\mathbf{g}}(t_s)$ about the Earth's axis by the angle $\omega(t - t_s)$.

3.1.2 Expressing the Necessary Rotations via GA

How might we formulate in GA terms the rotations that we described in the previous section? For the "sliding" along the solstice meridian, a reasonable idea is to define a unit bivector $\hat{\mathbf{M}}_s$ that's parallel to the plane containing that meridian, and whose positive sense is that of the rotation from $-\hat{\mathbf{r}}_s$ to

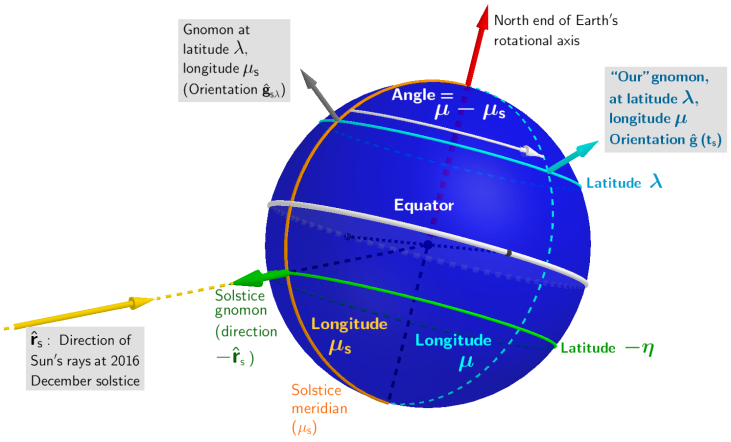

Figure 19: The third step in developing an expression for the orientation of "our" gnomon at any time: moving the $\hat{\mathbf{g}}_{s\lambda}$ gnomon along latitude λ longitude (μ) of our gnomon, whose orientation at the instant of the 2016 December solstice is $\hat{\mathbf{g}}(t_s)$.

$\hat{\mathbf{n}}_c$. Having defined $\hat{\mathbf{M}}_s$ in this way, $\hat{\mathbf{g}}_{s\lambda}$ is the rotation of $-\hat{\mathbf{r}}_s$ through the bivector angle $\hat{\mathbf{M}}_s(\lambda+\eta)$. (That is, through the scalar multiple $\lambda+\eta$ of the unit bivector $\hat{\mathbf{M}}_s$.) The representation of that rotation ([13], p. 89) would then be $Z_1 = e^{-\hat{\mathbf{M}}_s(\lambda+\eta)/2}$.

For the rotations about the Earth's axis, we'll define a unit vector $\hat{\mathbf{Q}}$ that's parallel to the equator. What should we choose as $\hat{\mathbf{Q}}$'s positive sense? The direction of the Earth's rotation about its axis is a good choice, all the more so because the dual of a $\hat{\mathbf{Q}}$ that's so defined is none other than the vector $\hat{\mathbf{n}}_c$. Using this definition of $\hat{\mathbf{Q}}$, the representation of the rotation of $\hat{\mathbf{g}}_{s\lambda}$ from the solstice meridian to our own meridian to the longitude of our meridian at time t_s is $Z_2 = e^{-\hat{\mathbf{Q}}(\mu-\mu_s)/2}$. The subsequent rotation of our meridian (and thus of our gnomon) from the time t_s to any other time t is represented by $Z_3 = e^{-\hat{\mathbf{Q}}\omega(t-t_s)/2}$.

Putting the preceding ideas together, we see that $\hat{\mathbf{g}}_L(t)$ is the result of the rotation of $-\hat{\mathbf{r}}_s$ by the composite of the three above-described rotations. As explained in [13], p. 125, the representation of that composite rotation is the product $Z_3Z_2Z_1$ of their respective rotations:

$$\begin{aligned} Z_3Z_2Z_1 &= \left\{e^{-\hat{\mathbf{Q}}\omega(t-t_s)/2}\right\}\left\{e^{-\hat{\mathbf{Q}}(\mu-\mu_s)/2}\right\}\left\{e^{-\hat{\mathbf{M}}_s(\lambda+\eta)/2}\right\} \\ &= \left\{e^{-\hat{\mathbf{Q}}[\mu-\mu_s+\omega(t-t_s)]/2}\right\}\left\{e^{-\hat{\mathbf{M}}_s(\lambda+\eta)/2}\right\}. \end{aligned}$$

To make that result more convenient, we'll define $k(\mu,t) = \mu - \mu_s + \omega(t-t_s)$, giving

$$Z_3Z_2Z_1 = \left\{e^{-\hat{\mathbf{Q}}k(\mu,t)/2}\right\}\left\{e^{-\hat{\mathbf{M}}_s(\lambda+\eta)/2}\right\}$$

Because that result is the representation of the rotation that produces $\hat{\mathbf{g}}_L(t)$

from $-\hat{r}_s$,

$$\hat{\mathbf{g}}_L(t) = \left\{e^{-\hat{\mathbf{Q}}k(\mu,t)/2}\right\}\left\{e^{-\hat{\mathbf{M}}_s(\lambda+\eta)/2}\right\}\left[-\hat{\mathbf{r}}_s\right]\left\{e^{\hat{\mathbf{M}}_s(\lambda+\eta)/2}\right\}\left\{e^{\hat{\mathbf{Q}}k(\mu,t)/2}\right\}$$

The above having been said, we're under no obligation to calculate $\hat{\mathbf{g}}_L(t)$ directly from $\hat{\mathbf{r}}_s$. Depending upon the complexity of the expressions that arise when we make substitutions for $\hat{\mathbf{r}}_s$, $\hat{\mathbf{M}}_s$, and $\hat{\mathbf{Q}}$, we might instead choose to first derive an expression for $\hat{\mathbf{g}}_{s\lambda}$ from $\hat{\mathbf{r}}_s$,

$$\hat{\mathbf{g}}_{s\lambda} = \left\{e^{-\hat{\mathbf{M}}_s(\lambda+\eta)/2}\right\}\left[-\hat{\mathbf{r}}_s\right]\left\{e^{\hat{\mathbf{M}}_s(\lambda+\eta)/2}\right\}, \tag{3.1}$$

after which we would calculate $\hat{\mathbf{g}}_L(t)$ via

$$\hat{\mathbf{g}}_L(t) = \left\{e^{-\hat{\mathbf{Q}}k(\mu,t)/2}\right\}\left[\hat{\mathbf{g}}_{s\lambda}\right]\left\{e^{\hat{\mathbf{Q}}k(\mu,t)/2}\right\}. \tag{3.2}$$

Other reasons for choosing this route include the possibility of gaining greater insight into the relationships between the calculations and the physical phenomena, and the desire to check the results of each step to make sure that they make sense.

3.1.3 Formulating the Bivectors Needed for the Rotations

In the previous section, we used GA's capacities for formulating rotations to express $\hat{\mathbf{g}}_L(t)$ in terms of the vector $\hat{\mathbf{r}}_s$ $(= \hat{\mathbf{r}}(t_s))$ and the time-invariant bivectors $\hat{\mathbf{M}}_s$ and $\hat{\mathbf{Q}}$. Now, let's develop expressions for those bivectors in terms of the vectors $\hat{\mathbf{a}}$ and $\hat{\mathbf{b}}$ of the Earth's Kepler orbit. Our purpose in doing so is to facilitate the numerical calculations of $\alpha(t)$ and $\beta(t)$ that we will wish to make.

$\hat{\mathbf{a}} \wedge \hat{\mathbf{b}} = \hat{\mathbf{a}}\hat{\mathbf{b}}$ because $\hat{\mathbf{a}} \perp \hat{\mathbf{b}}$.

In Fig. 20, we introduce the unit bivector $\hat{\mathbf{C}}$ $\left(= \hat{\mathbf{a}} \wedge \hat{\mathbf{b}} = \hat{\mathbf{a}}\hat{\mathbf{b}}\right)$. It's parallel to the ecliptic plane, and its positive sense is in the direction of the Earth's orbit. Thus, for any time t,

$$\begin{aligned}\hat{\mathbf{r}}(t) &= \left[e^{-\hat{\mathbf{C}}\theta(t)/2}\right]\left[\hat{\mathbf{a}}\right]\left[e^{\hat{\mathbf{C}}\theta(t)/2}\right] \\ &= \hat{\mathbf{a}}e^{\hat{\mathbf{C}}\theta(t)},\end{aligned} \tag{3.3}$$

because $\hat{\mathbf{a}}$ is parallel to $\hat{\mathbf{C}}$. In particular, $\hat{\mathbf{r}}_s = \hat{\mathbf{a}}e^{\hat{\mathbf{C}}\theta_s}$.

We decided in the previous section to define $\hat{\mathbf{M}}_s$ as the unit bivector that is parallel to the solstice meridian, and whose positive sense is in the direction of the rotation from $-\hat{\mathbf{r}}_s$ $\hat{\mathbf{n}}_c$. Examining Figs. 21–22, we see that those characteristics are possessed by the bivector $(-\hat{\mathbf{r}}_s) \wedge \hat{\mathbf{c}}$, where $\hat{\mathbf{c}}$ is $\hat{\mathbf{C}}$'s dual. Comparing Figs. 20 and 22, we also see that the set of vectors $\left\{\hat{\mathbf{a}}, \hat{\mathbf{b}}, \hat{\mathbf{c}}\right\}$ forms a right-handed, orthonormal basis—quite a favorable development for our purposes. Thus, we define

$$\begin{aligned}\hat{\mathbf{M}}_s &= (-\hat{\mathbf{r}}_s) \wedge \hat{\mathbf{c}} \\ &= -\hat{\mathbf{r}}_s\hat{\mathbf{c}},\end{aligned} \tag{3.4}$$

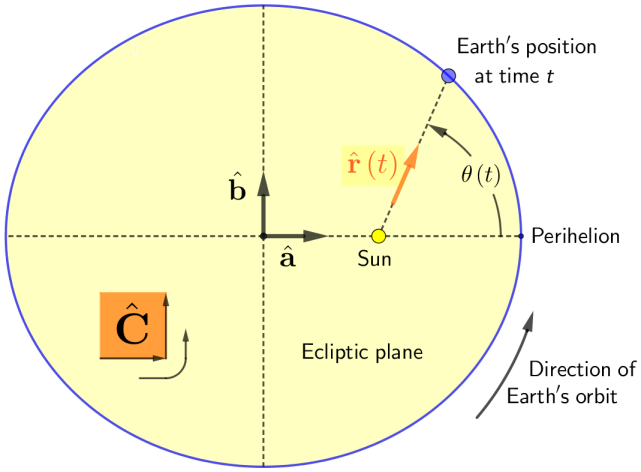

Figure 20: Schematic diagram of the Earth's Kepler orbit, showing the vectors $\hat{\mathbf{a}}$ and $\hat{\mathbf{b}}$ along with the unit bivector $\hat{\mathbf{C}}$ $\left(= \hat{\mathbf{a}} \wedge \hat{\mathbf{b}} = \hat{\mathbf{a}}\hat{\mathbf{b}}\right)$. The arrow next to the square representing $\hat{\mathbf{C}}$ shows $\hat{\mathbf{C}}$'s positive sense. Because that sense is in the direction of the Earth's orbit, $\hat{\mathbf{r}}(t) = \hat{\mathbf{a}} e^{\hat{\mathbf{C}}\theta(t)}$.

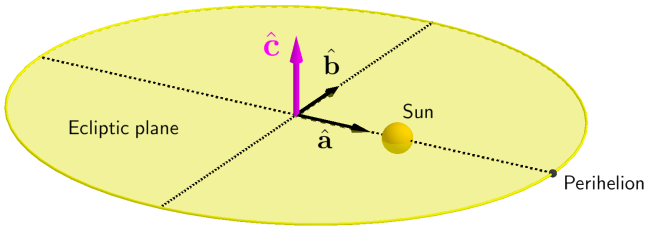

Figure 21: Definition of the vector $\hat{\mathbf{c}}$ that we will use in formulating $\hat{\mathbf{M}}_s$. The set of vectors $\left\{\hat{\mathbf{a}}, \hat{\mathbf{b}}, \hat{\mathbf{c}}\right\}$ forms a right-handed, orthonormal basis.

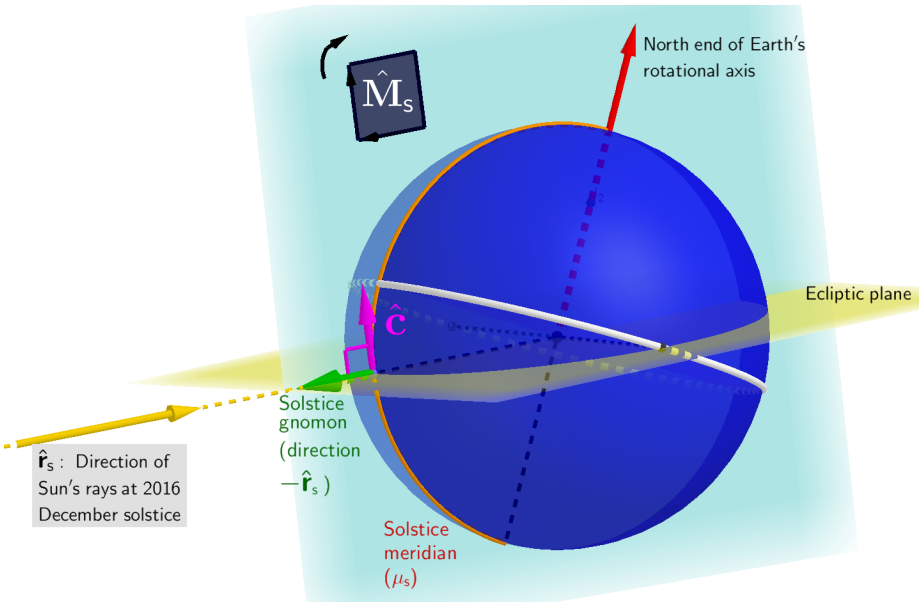

Figure 22: Illustrating the use of $\hat{\mathbf{c}}$, which is $\hat{\mathbf{C}}$'s dual. The bivector $(-\hat{\mathbf{r}}_s) \wedge \hat{\mathbf{c}}$ has the characteristics that we specified earlier for $\hat{\mathbf{M}}_s$. The arrow next to the square representing $\hat{\mathbf{M}}_s$ shows $\hat{\mathbf{M}}_s$'s positive sense.

because $\hat{\mathbf{r}}_s \perp \hat{\mathbf{c}}$.

With $\hat{\mathbf{M}}_s$ defined in this way, $\hat{\mathbf{Q}}$, which we need for rotations about the Earth's axis, is just the rotation of $\hat{\mathbf{C}}$ through the bivector angle $\hat{\mathbf{M}}\eta$ Fig. 23:

$$\hat{\mathbf{Q}} = \left[e^{-\hat{\mathbf{M}}_s \eta/2}\right] \left[\hat{\mathbf{C}}\right] \left[e^{\hat{\mathbf{M}}_s \eta/2}\right]. \tag{3.5}$$

3.1.4 Celestial North: $\hat{\mathbf{n}}_c$

From Fig. 23, we can see that the rotation from $\hat{\mathbf{c}}$ to $\hat{\mathbf{n}}_c$ is the same as that from $\hat{\mathbf{M}}_s$ to $\hat{\mathbf{Q}}$. Therefore, having formulated $\hat{\mathbf{M}}_s$, we can now express $\hat{\mathbf{n}}_c$ readily as the rotation of $\hat{\mathbf{c}}$ by the bivector angle $\hat{\mathbf{M}}_s\eta$:

$$\hat{\mathbf{n}}_c = \left[e^{-\hat{\mathbf{M}}_s \eta/2}\right] [\hat{\mathbf{c}}] \left[e^{\hat{\mathbf{M}}_s \eta/2}\right]. \tag{3.6}$$

We could also formulate it as dual of $\hat{\mathbf{Q}}$.

3.2 Our Model, in Words and in GA Terms

We developed our model and defined its variables in the course of "puzzling-through" the gnomon problem, so we should take time now to summarize and organize (Table 2) before moving on to derive equations for the angles α and β.

Table 2: Summary of the quantities in our model.

Symbol	Description
$\left\{\hat{\mathbf{a}}, \hat{\mathbf{b}}, \hat{\mathbf{c}}\right\}$	The right-handed, orthonormal basis of our reference system.
t	Time, per Kepler equation. When $t = 0$, Earth is at perihelion.
t_s	Value of t at the instant of the 2016 December solstice.
η	The angle of the equator with respect to the ecliptic. Positive if in the positive sense of $\hat{\mathbf{M}}_s$.
λ	Our (that is, our gnomon's) latitude. Positive in the Northern Hemisphere, negative in the Southern Hemisphere.
μ	Our longitude, with East longitudes taken as positive.
μ_s	Value of μ for the "solstice meridian": that which faced the Sun directly at the December 2016 solstice.
ω	Angular velocity of the Earth's rotation about its own axis.
$k(\mu, t)$	$= \mu - \mu_s + \omega(t - t_s)$.
$\mathbf{r}(t)$	Vector from Sun's center to Earth's center at time t. Direction of Sun's rays is approximated as equal to $\hat{\mathbf{r}}(t)$.
$\hat{\mathbf{r}}_s$	$= \hat{\mathbf{r}}(t_s)$.
$\theta(t)$	Angle from $\hat{\mathbf{a}}$ to $\hat{\mathbf{r}}(t)$. Positive in the direction of the Earth's orbit, and thus if in the positive sense of $\hat{\mathbf{C}}$.
θ_s	$= \theta(t_s)$.
$\hat{\mathbf{C}}$	Unit bivector $\left(= \hat{\mathbf{a}}\hat{\mathbf{b}}\right)$ of the ecliptic plane. Assumed constant.
$\hat{\mathbf{M}}_s$	Unit bivector of the solstice meridian. Equal to $-\hat{\mathbf{r}}_s\hat{\mathbf{c}}$.
$\hat{\mathbf{Q}}$	Unit bivector of Earth's equatorial plane. Assumed constant; equal to rotation of $\hat{\mathbf{Q}}$ by $\hat{\mathbf{M}}_s\eta$
$\hat{\mathbf{n}}_c$	"Celestial North": the direction from the center of the Earth to the Geographic North Pole.
$\hat{\mathbf{n}}_L(t)$	"Local north": the direction, at t, of "north" at our location.
$\hat{\mathbf{g}}_{s\lambda}$	Direction, at time t_s, of a gnomon at latitude λ, longitude μ_s.
$\hat{\mathbf{g}}_L(t)$	Direction, t, from base of our gnomon to its tip. This vector is $\hat{\mathbf{T}}(t)$'s dual.
$\hat{\mathbf{T}}(t)$	Unit bivector parallel to the plane that, at time t, is tangent to Earth's surface at base of our gnomon. $\hat{\mathbf{T}}(t)$'s dual is $\hat{\mathbf{g}}_L(t)$.
$\hat{\mathbf{s}}(t)$	Direction, at time t, from base of our gnomon to tip of its shadow.
$\alpha(t)$	Angle between gnomon's shaft and Sun's rays at instant t.
$\beta(t)$	Angle of rotation from $\hat{\mathbf{n}}_L(t)$ to $\hat{\mathbf{s}}(t)$.

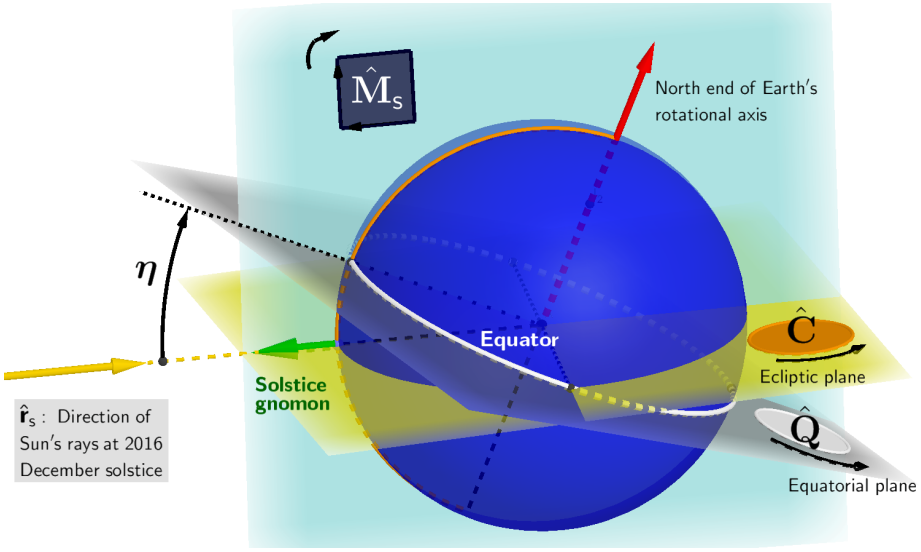

Figure 23: $\hat{\mathbf{Q}}$ is the rotation of $\hat{\mathbf{C}}$ through the bivector angle $\hat{\mathbf{M}}\eta$.

Our model is that the Earth is perfectly spherical, and orbits the Sun according to the Kepler model. The direction of the Sun's rays is the same as the direction $\hat{\mathbf{r}}(t)$ from the center of the Sun to the center of the Earth. The Earth's equatorial plane is inclined by angle η (assumed constant) with respect to the ecliptic. The Earth rotates at constant angular velocity ω. At the instant of the 2016 December solstice, the longitude that faces the Sun directly is μ_s. Our gnomon is located at latitude λ, longitude μ, and casts a shadow upon a plane that is tangent to the Earth at that same location.

We wish to be able to calculate, for any time t, the angle between the Sun's rays and the gnomon, and the angle between the direction "local north" and the gnomon's shadow.

In GA terms (Fig. 24), vector $\hat{\mathbf{g}}_L(t)$ rotates at constant angular velocity $\hat{\mathbf{Q}}\omega$. The vector $\hat{\mathbf{r}}(t)$ varies with time according to the Kepler equation ((2.1)). Vector $\hat{\mathbf{n}}_c$ is the dual of $\hat{\mathbf{Q}}$. Vector $\hat{\mathbf{g}}_L(t)$ is the dual of bivector $\hat{\mathbf{T}}(t)$.

We wish to be able to calculate, for any time t, (1) the angle between the vectors $\hat{\mathbf{g}}_L(t)$ and $\hat{\mathbf{r}}(t)$, and (2) the angle of rotation from $\hat{\mathbf{n}}_c$'s projection upon $\hat{\mathbf{T}}(t)$ to $\hat{\mathbf{r}}(t)$'s projection upon $\hat{\mathbf{T}}(t)$.

4 Derivations of Formulas

Several of the derivations use formulas that are developed in Section 2.3.2, and implemented in Maxima in [14].

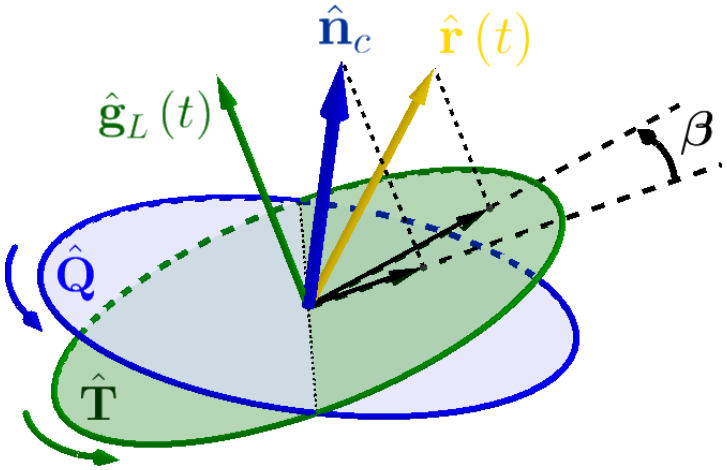

Figure 24: The model, in GA terms. Arrows show the positive senses of the bivectors $\hat{\mathbf{Q}}$ and $\hat{\mathbf{T}}$. Vector $\hat{\mathbf{g}}_L\,(t)$ rotates at constant angular velocity $\hat{\mathbf{Q}}\omega$. The vector $\hat{\mathbf{r}}\,(t)$ varies with time according to the Kepler equation ((2.1)). Vector $\hat{\mathbf{n}_c}$ is the dual of $\hat{\mathbf{Q}}$. Vector $\hat{\mathbf{g}}_L\,(t)$ is the dual of bivector $\hat{\mathbf{T}}\,(t)$. Not shown is the angle α between $-\hat{\mathbf{g}}_L\,(t)$ and $\hat{\mathbf{r}}\,(t)$.

4.1 $\hat{\mathbf{r}}\,(t)$, $\hat{\mathbf{r}}_s$

This vector is the rotation of $\hat{\mathbf{a}}$ through the bivector angle $\hat{\mathbf{C}}\theta\,(t)$. Thus (Eq. (3.3)),

$$\begin{aligned}\hat{\mathbf{r}}\,(t) &= \mathbf{a}e^{\hat{\mathbf{C}}\theta(t)} \\ &= \hat{\mathbf{a}}e^{\hat{\mathbf{a}}\hat{\mathbf{b}}\theta(t)} \\ &= \hat{\mathbf{a}}\left[\cos\theta\,(t) + \hat{\mathbf{a}}\hat{\mathbf{b}}\sin\theta\,(t)\right] \\ &= \hat{\mathbf{a}}\cos\theta\,(t) + \hat{\mathbf{b}}\sin\theta\,(t)\,. \end{aligned} \tag{4.1}$$

Specifically,

$$\hat{\mathbf{r}}_s = \hat{\mathbf{r}}\,(t_s) = \hat{\mathbf{a}}\cos\theta_s + \hat{\mathbf{b}}\sin\theta_s. \tag{4.2}$$

4.2 $\hat{\mathbf{M}}_s$

From Eq. (3.4), $\hat{\mathbf{M}}_s = -\hat{\mathbf{r}}_s\hat{\mathbf{c}}$. Thus, using the expression for $-\hat{\mathbf{r}}_s$ from Eq. (4.2),

$$\begin{aligned}\hat{\mathbf{M}}_s &= -\left[\hat{\mathbf{a}}\cos\theta_s + \hat{\mathbf{b}}\sin\theta_s\right]\hat{\mathbf{c}} \\ &= -\hat{\mathbf{b}}\hat{\mathbf{c}}\sin\theta_s - \hat{\mathbf{a}}\hat{\mathbf{c}}\cos\theta_s. \end{aligned} \tag{4.3}$$

$\hat{\mathbf{M}}_s$ is also the rotation of the bivector $\hat{\mathbf{c}}\hat{\mathbf{a}}$ through the bivector angle $\hat{\mathbf{Q}}\theta_s$:

$$\begin{aligned}\hat{\mathbf{M}}_s &= \left[e^{-\mathbf{C}\frac{\theta_s}{2}}\right][\hat{\mathbf{c}}\hat{\mathbf{a}}]\left[e^{\mathbf{C}\frac{\theta_s}{2}}\right] \\ &= \left[\cos\tfrac{\theta_s}{2} - \hat{\mathbf{a}}\hat{\mathbf{b}}\sin\tfrac{\theta_s}{2}\right][\hat{\mathbf{c}}\hat{\mathbf{a}}]\left[\cos\tfrac{\theta_s}{2} + \hat{\mathbf{a}}\hat{\mathbf{b}}\sin\tfrac{\theta_s}{2}\right] \\ &= -\hat{\mathbf{b}}\hat{\mathbf{c}}\sin\theta_s - \hat{\mathbf{a}}\hat{\mathbf{c}}\cos\theta_s.\end{aligned}$$

4.3 $\hat{\mathbf{n}}_c$

This vector is the rotation of $\hat{\mathbf{c}}$ by the bivector angle $\hat{\mathbf{M}}_s\eta$. We'll calculate $\hat{\mathbf{n}}_c$ using Eqs. (2.7) and (2.8). To do so, we need to write the representation of the rotation by $\hat{\mathbf{M}}_s\eta$ in the form $f_o - \left(\hat{\mathbf{a}}\hat{\mathbf{b}}f_{ab} + \hat{\mathbf{b}}\hat{\mathbf{c}}f_{bc} + \hat{\mathbf{a}}\hat{\mathbf{c}}f_{ac}\right)$:

$$\begin{aligned}e^{-\hat{\mathbf{M}}_s\frac{\eta}{2}} &= \cos\tfrac{\eta}{2} - \left(-\hat{\mathbf{b}}\hat{\mathbf{c}}\sin\theta_s - \hat{\mathbf{a}}\hat{\mathbf{c}}\cos\theta_s\right)\sin\tfrac{\eta}{2} \\ &= \cos\tfrac{\eta}{2} - \left(\hat{\mathbf{b}}\hat{\mathbf{c}}\sin\theta_s\sin\tfrac{\eta}{2} - \hat{\mathbf{a}}\hat{\mathbf{c}}\cos\theta_s\sin\tfrac{\eta}{2}\right),\end{aligned} \tag{4.4}$$

so $f_o = \cos\frac{\eta}{2}$, $f_{ab} = 0$, $f_{bc} = -\sin\theta_s\sin\frac{\eta}{2}$, and $f_{ac} = -\cos\theta_s\sin\frac{\eta}{2}$. Therefore,

$$\begin{aligned}\hat{\mathbf{n}}_c = &\hat{\mathbf{a}}\sin(\eta)\cos\theta_s \\ &+ \hat{\mathbf{b}}\sin(\eta)\sin\theta_s \\ &+ \hat{\mathbf{c}}\cos(\eta).\end{aligned} \tag{4.5}$$

4.4 $\hat{\mathbf{g}}_{s\lambda}$

The vector $\hat{\mathbf{g}}_{s\lambda}$ is the rotation of $-\hat{\mathbf{r}}_s$ by the bivector angle $\hat{\mathbf{M}}_s\,(\eta+\lambda)$. As was the case for calculating $\hat{\mathbf{n}}_c$, we need to write the representation of our rotation in the form $f_o - \left(\hat{\mathbf{a}}\hat{\mathbf{b}}f_{ab} + \hat{\mathbf{b}}\hat{\mathbf{c}}f_{bc} + \hat{\mathbf{a}}\hat{\mathbf{c}}f_{ac}\right)$:

$$\begin{aligned}e^{-\hat{\mathbf{M}}_s\frac{\eta+\lambda}{2}} &= \cos\tfrac{\eta+\lambda}{2} - \left(-\hat{\mathbf{b}}\hat{\mathbf{c}}\sin\theta_s - \hat{\mathbf{a}}\hat{\mathbf{c}}\cos\theta_s\right)\sin\tfrac{\eta+\lambda}{2} \\ &= \cos\tfrac{\eta+\lambda}{2} - \left(\hat{\mathbf{b}}\hat{\mathbf{c}}\sin\theta_s\sin\tfrac{\eta+\lambda}{2} - \hat{\mathbf{a}}\hat{\mathbf{c}}\cos\theta_s\sin\tfrac{\eta+\lambda}{2}\right),\end{aligned} \tag{4.6}$$

so $f_o = \cos\frac{\eta+\lambda}{2}$, $f_{ab} = 0$, $f_{bc} = -\sin\theta_s\sin\frac{\eta+\lambda}{2}$, and $f_{ac} = -\cos\theta_s\sin\frac{\eta+\lambda}{2}$. Therefore,

$$\begin{aligned}\hat{\mathbf{g}}_{s\lambda} = &\hat{\mathbf{a}}\left[-\cos\theta_s\cos\left(\eta+\lambda\right)\right] \\ &+ \hat{\mathbf{b}}\left[-\sin\theta_s\cos\left(\eta+\lambda\right)\right] \\ &+ \hat{\mathbf{c}}\left[\sin\left(\eta+\lambda\right)\right].\end{aligned} \tag{4.7}$$

4.5 $\hat{\mathbf{Q}}$

$\hat{\mathbf{Q}}$ is $\hat{\mathbf{C}}$ rotated through the bivector angle $\hat{\mathbf{M}}_s\eta$:

$$\begin{aligned}\hat{\mathbf{Q}} &= \left[e^{-\hat{\mathbf{M}}_s\frac{\eta}{2}}\right]\left[\hat{\mathbf{C}}\right]\left[e^{\hat{\mathbf{M}}_s\frac{\eta}{2}}\right] \\ &= \left[\cos\tfrac{\eta}{2} - \left(-\hat{\mathbf{b}}\hat{\mathbf{c}}\sin\theta_s - \hat{\mathbf{a}}\hat{\mathbf{c}}\cos\theta_s\right)\sin\tfrac{\eta}{2}\right]\left[\hat{\mathbf{a}}\hat{\mathbf{b}}\right]\left[\cos\tfrac{\eta}{2} + \left(-\hat{\mathbf{b}}\hat{\mathbf{c}}\sin\theta_s - \hat{\mathbf{a}}\hat{\mathbf{c}}\cos\theta_s\right)\sin\tfrac{\eta}{2}\right] \\ &= \hat{\mathbf{a}}\hat{\mathbf{b}}\cos\eta + \hat{\mathbf{b}}\hat{\mathbf{c}}\cos\theta_s\sin\eta - \hat{\mathbf{a}}\hat{\mathbf{c}}\sin\theta_s\sin\eta. \end{aligned} \tag{4.8}$$

4.6 Our Gnomon's Direction: $\hat{\mathbf{g}}_L(t)$

This vector is the rotation of $\hat{\mathbf{g}}_{s\lambda}$ by the bivector angle $\hat{\mathbf{Q}}k(\mu,t)$. The parameters of our rotation are $f_0 = \cos\dfrac{k(\mu,t)}{2}$, $f_{ab} = \cos\eta\sin\dfrac{k(\mu,t)}{2}$, $f_{bc} = \cos\theta_s\sin(\eta)\sin\dfrac{k(\mu,t)}{2}$, $f_{ac} = -\sin\theta_s\sin(\eta)\sin\dfrac{k(\mu,t)}{2}$. Therefore, from Eqs. (2.7) and (2.8),

$$\begin{aligned}\hat{\mathbf{g}}_L(t) = {}& \hat{\mathbf{a}}\{\sin\theta_s\cos\lambda\sin k(\mu,t) - \cos\theta_s\cos(\eta+\lambda) + \cos\theta_s\cos\eta\cos\lambda[1-\cos k(\mu,t)]\} \\ &+\hat{\mathbf{b}}\{\sin\theta_s\cos\eta\cos\lambda[1-\cos k(\mu,t)] - \sin\theta_s\cos(\eta+\lambda) - \cos\theta_s\cos\lambda\sin k(\mu,t)\} \\ &+\hat{\mathbf{c}}\{\sin(\eta+\lambda) - \sin\eta\cos\lambda[1-\cos k(\mu,t)]\}.\end{aligned} \tag{4.9}$$

4.7 The Angle $\alpha(t)$

As noted in Section 2.4, $\alpha(t)$ is the angle of rotation from $\bar{\hat{\mathbf{g}}}_L(t)$ to $\hat{\mathbf{r}}(t)$. A gnomon is a device for producing shadows, which occur only when the Sun is above the horizon; in other words, when the inner product of $\bar{\hat{\mathbf{g}}}_L(t)\cdot\hat{\mathbf{r}}(t)$ is positive. Having ensured that, the only characteristic of $\alpha(t)$ that interests us is its magnitude. Therefore, all we need to know is $\alpha(t)$'s cosine, which is equal to the inner product $\hat{\mathbf{u}}\cdot\hat{\mathbf{v}}$. Therefore, $\cos\alpha(t) = [\bar{\hat{\mathbf{g}}}_L(t)]\cdot\hat{\mathbf{r}}(t)$. We've developed expressions for these two vectors (Eqs. (4.9) and (4.1), we find that

$$\begin{aligned}\cos\alpha = {}& \{\cos(\eta+\lambda) - \cos\eta\cos\lambda[1-\cos k(\mu,t)]\}\cos(\theta_t-\theta_s) \\ &+ \cos\lambda\sin(\theta_t-\theta_s)\sin k(\mu,t).\end{aligned} \tag{4.10}$$

Some comments upon that equation: At the instant t_s of the December solstice, $\theta(t) = \theta_s$. In addition, for points along the meridian that's aligned with the Sun at that time (e.g., points along $\mathbf{M}_s$), $k(\mu,t) = 0$. Therefore, along that meridian and at that instant, Eq. (4.10) reduces to $\cos\alpha(t_s) = \cos(\eta+\lambda)$.

Does that result make sense? Does our answer make sense?

4.8 The Angle $\beta(t)$

We will find $\beta(t)$ from its sine and cosine, which we will calculate according to Section 2.3.3.

4.8.1 Denominator of the sine and cosine of $\beta(t)$

This denominator is the product of $\|\hat{\mathbf{n}}_c \cdot \hat{\mathbf{T}}(t)\|$ and $\|[\hat{\mathbf{r}}(t)] \cdot \hat{\mathbf{T}}(t)\|$. We'll treat each of those quantities in turn.

The norm $\|\hat{\mathbf{n}}_c \cdot \hat{\mathbf{T}}(t)\|$. To calculate this norm, we will use Eq. (2.12), which expresses the norm of a vector's projection upon a bivector in terms of that bivector's dual. In our case, the dual of $\hat{\mathbf{T}}(t)$ is $\hat{\mathbf{g}}_L(t)$ (Eq. (4.9)), and $\hat{\mathbf{n}}_c$ is given by Eq. (4.3). The result, as given in [14], is $\|\hat{\mathbf{n}}_c \cdot \hat{\mathbf{T}}(t)\| = |\cos\lambda|$. However, $|\cos\lambda| = \cos\lambda$ in our model because $-\pi/2 \leq \lambda \leq \pi/2$. Thus,

$$\|\hat{\mathbf{n}}_c \cdot \hat{\mathbf{T}}(t)\| = \cos\lambda. \tag{4.11}$$

Does our answer make sense?

A surprisingly simple result. Does it make sense? Let's look at Fig. 14. We can deduce that the angle between $\hat{\mathbf{n}}_c$ and $\hat{\mathbf{T}}(t)$ is either λ or $180° + \lambda$. Because $\hat{\mathbf{n}}_c$ is a unit vector, the magnitude of $\mathsf{R}_{\hat{\mathbf{T}}}(\hat{\mathbf{n}}_c)$ (i.e., of $\hat{\mathbf{n}}_c$'s projection upon $\hat{\mathbf{T}}(t)$) is indeed $\cos\lambda$. As explained in [12], $\hat{\mathbf{n}}_c \cdot \hat{\mathbf{T}}(t)$ evaluates to a vector that is a 90° rotation of $\mathsf{R}_{\hat{\mathbf{T}}}(\hat{\mathbf{n}_c})$, with no change in the latter's magnitude. Therefore, $\|\hat{\mathbf{n}}_c \cdot \hat{\mathbf{T}}(t)\| = \|\mathsf{R}_{\hat{\mathbf{T}}}(\hat{\mathbf{n}}_c)\| = \cos\lambda$.

The norm $\|[\hat{\mathbf{r}}(t)] \cdot \hat{\mathbf{T}}(t)\|$ As shown in [14], using (4.1)'s expression for $\hat{\mathbf{r}}(t)$ in Eq. (2.12) yields a result that I was not able to reduce to a simple form. Nor was I able to do so by starting from the observation that because $\hat{\mathbf{r}}(t)$ is a unit vector,

$$\|[\hat{\mathbf{r}}(t)] \cdot \hat{\mathbf{T}}(t)\|^2 = 1 - \{[\hat{\mathbf{r}}(t)] \cdot [\hat{\mathbf{g}}_L(t)]\}^2,$$

from which ([14])

$$\begin{aligned}\|[\hat{\mathbf{r}}(t)] \cdot \hat{\mathbf{T}}(t)\|^2 = 1 - \{&[\cos\eta\cos\lambda(1 - \cos k(\mu,t)) - \cos(\eta+\lambda)]\cos[\theta_t - \theta_s] \\ &- \cos\lambda\sin k(\mu,t)\sin[\theta(t) - \theta_s]\}^2.\end{aligned} \tag{4.12}$$

Does our answer make sense? What should $\|[\hat{\mathbf{r}}(t)] \cdot \hat{\mathbf{T}}(t)\|$ be when $t = t_s$? Note that when $t = t_s$, $\theta_t = \theta_s$ and $k(\mu,t) = 0$.

4.8.2 Numerators of $\sin\beta(t)$ and $\cos\beta(t)$

Eqs. (4.5), (4.1), and (4.9) (respectively) present the expressions that we developed for $\hat{\mathbf{n}}_c$, $\hat{\mathbf{r}}(t)$, and $\hat{\mathbf{g}}_L(t)$. To calculate the numerators of $\sin\beta(t)$ and $\cos\beta(t)$, we will substitute those expressions for (respectively)$\mathbf{u}$, $\mathbf{v}$, and $\hat{\mathbf{e}}$ in Eqs. (2.11) and (2.14). Those equations are implemented in [14], which is the source from which we cite the results presented in the paragraphs that follow.

Note that $\cos\lambda$ (which is $\|\hat{\mathbf{n}}_c \cdot \hat{\mathbf{T}}(t)\|$, Eq. (4.11)) is a factor of every term in both numerators.

Numerator of $\sin\beta(t)$ As given in [12], the numerator of $\sin\beta(t)$ is

$$\begin{aligned} Numerator\ of\ \sin\beta(t) = &\cos\lambda\cos k(\mu,t)\sin[\theta(t)-\theta_s] \\ &-\cos\eta\cos\lambda\sin k(\mu,t)\cos[\theta(t)-\theta_s]. \end{aligned} \tag{4.13}$$

Numerator of $\cos\beta(t)$ As given in [12], the numerator of $\sin\beta$ is

$$\begin{aligned} Numerator\ of\ \cos\beta(t) = &\cos\lambda\sin\lambda\sin k(\mu,t)\sin[\theta(t)-\theta_s] \\ &+\cos\eta\cos\lambda\sin\lambda\cos k(\mu,t)\cos[\theta(t)-\theta_s] \\ &+\sin\eta\cos^2\lambda\cos[\theta(t)-\theta_s]. \end{aligned} \tag{4.14}$$

5 Validation of the Model and Calculations

We'll validate the model and calculations in two ways: (1) by deducing, from mathematical analyses of our equations for $\alpha(t)$ and $\beta(t)$, the latitudes at which solar zeniths occur on the equinoxes and solstices, and the azimuths at which the Sun sets on those dates; and (2) by making numerical predictions of the Sun's azimuth and altitude as seen at specific times from Port Moresby, Papua New Guinea, and from San Cristóbal de Las Casas, Chiapas, Mexico.

Those locations were chosen because they lie on opposite sides of the equator, and also on opposite sides of the meridian that faces the Sun at the instant of the December 2016 solstice. Thus, their values of λ and $\mu - \mu_s$ are of opposite algebraic signs (Fig. 25). For that reason, they provide a way of detecting sign errors in our calculations. Because the two cities also lie within the Tropics of their respective hemispheres, the Sun will be in the northern half of the sky during one part of the year, and in the southern half during the other. That characteristic will enable us to detect other types of errors, if present.

5.0.1 Data for Earth's Orbit, the December 2016 Solstice, Port Moresby, and San Cristóbal de Las Casas

The Earth and its orbit Reference [5] gives the orbit's eccentricity (ϵ) as 0.1671022, and its orbital period, T, 365.242 tropical days.

The inclination of the Earth's rotational axis is 23.44°. At the December solstice, the axis is pointed away from the Sun, so the algebraic sign of that angle is positive. Thus, $\eta = 23.44°$. Identifying the Earth's rotational angular velocity, ω, requires some thought. As noted in [8], the Earth rotates by slightly more than 360° during one tropical day. Over the course of a full year, that slight

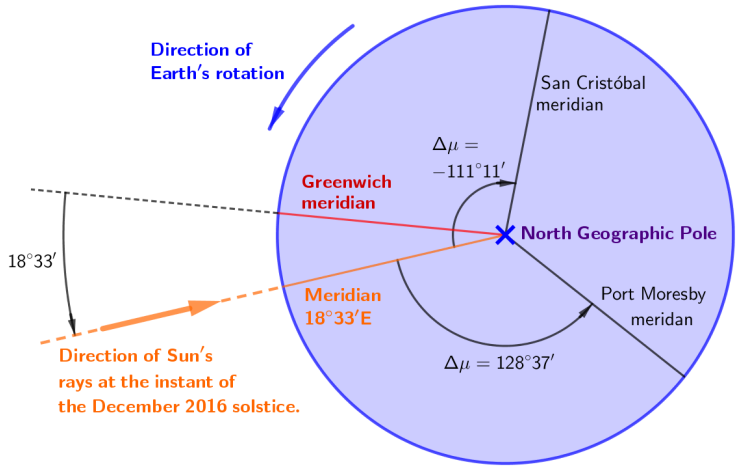

Figure 25: Relative positions of the meridians of Port Moresby and San Cristóbal de Las Casas with respect to the Greenwich Meridian and the meridian that faces the Sun directly at the instant of the December 2016 solstice. Note that $\Delta\mu = \mu - \mu_s$.

daily excess adds up to one full rotation. Therefore, the Earth makes 366.242 rotations of 2π radians each in 365.242 tropical days, from which $\omega = 6.3004$ radians/tropical day.

The December 2016 solstice Reference [7] found that for the December 2016 solstice, which occurred at UTC 21 December 2016 10:44:44, $\theta_s = -0.230099$ radians, and $t_s = -12.9379$ tropical days. Using the planetarium program Stellarium ([3]), I found that the meridian of longitude that faced the Sun directly at the instant of the solstice was E 18°33′ (-0.32376 radians, according to the sign convention used in our model): approximately that of Stockholm, Sweden and Cape Town, Republic of South Africa.

Port Moresby and San Cristóbal de Las Casas According to [3], Port Moresby's latitude and longitude are S9°26′35.30″ E147°10′46.98″, while San Cristóbal's are N16°44′12.00″ W92°38′18.01″. Therefore, Port Moresby's value of $\mu - \mu_s$ is +128°37′, or 2.2450 radians, and San Cristóbal´s is -1.9406 radians.

Summary of the parameters used in validating the model Tables 3 and 4 summarize the relevant data.

Table 3: Summary of the parameters used in validating the model. "Days" are tropical days. The quantity "$\Delta\mu$ is $\mu - \mu_s$.

Parameters of the Earth and its orbit

ϵ	T, days	η, radians	ω, radians/day
0.16710	365.242	0.40911	6.30039

Parameters of the December 2016 solstice

Date (UTC)	θ_s, radians	t_s, days	μ_s, radians
21/12/2016 10:44:00	-0.23010	-12.938	0.32376

Parameters of Port Moresby and San Cristóbal de Las Casas

	λ, radians	$\Delta\mu$, radians
Port Moresby	-0.16481	2.2450
San Cristóbal	0.29211	-1.9406

Table 4: Times and dates of solstices and equinoxes for the year 2017, and the number of tropical days between each event and the December 2016 solstice. (Adapted and corrected from [7].)

Event	UTC Time and date ([4])	$t - t_s$, days
Dec. 2016 solst	21/12/2016 10:44:00	0.000
Mar. 2017 equin	20/03/2017 10:29:00	88.987
June 2017 solst	21/06/2017 04:24:00	181.736
Sept. 2017 equin	22/09/2017 20:02:00	275.388
Dec. 2017 solst	21/12/2017 16:28:00	365.239

5.1 Predictions, from Mathematical Analyses of Formulas, about Solar Zeniths and the Sun's Azimuths at Sunrise and Sunset

For convenience, we'll repeat Eqs. (4.10), (4.13), and (4.14) here:

$$\begin{aligned}\cos\alpha(t) = {} & \{\cos(\eta+\lambda) - \cos\eta\cos\lambda\,[1-\cos k(\mu,t)]\}\cos(\theta_t-\theta_s) \\ & + \cos\lambda\sin(\theta_t-\theta_s)\sin k(\mu,t)\end{aligned} \tag{5.1}$$

$$\begin{aligned}Numerator\ of\ \sin\beta(t) = {} & \cos\lambda\cos k(\mu,t)\sin[\theta(t)-\theta_s] \\ & - \cos\eta\cos\lambda\sin k(\mu,t)\cos[\theta(t)-\theta_s]\,.\end{aligned} \tag{5.2}$$

$$\begin{aligned}Numerator\ of\ \cos\beta(t) = {} & \cos\lambda\sin\lambda\sin k(\mu,t)\sin[\theta(t)-\theta_s] \\ & + \cos\eta\cos\lambda\sin\lambda\cos k(\mu,t)\cos[\theta(t)-\theta_s] \\ & + \sin\eta\cos^2\lambda\cos[\theta(t)-\theta_s]\,.\end{aligned} \tag{5.3}$$

We'll also recall that from Eqs. (4.11) and (4.12), the denominator of $\sin\beta$ and $\cos\beta$ is the product of $\cos\lambda$ and the square root of

$$\begin{aligned}1 - \{ & [\cos\eta\cos\lambda\,(1-\cos k(\mu,t)) - \cos(\eta+\lambda)]\cos[\theta_t-\theta_s] \\ & - \cos\lambda\sin k(\mu,t)\sin[\theta(t)-\theta_s]\}^2\,.\end{aligned} \tag{5.4}$$

Now, we'll analyze those formulas to find out what they predict for the azimuths and latitudes of sunrises, sunsets, and solar zeniths. In some cases, we'll also find it useful to recognize that because we measure latitudes from the equator, the latitudes λ and $\pi-\lambda$ are in fact the same latitude (Fig. 26).

5.1.1 On the March Equinox: Sunrise, Sunset, and the Movement of the Shadow's Endpoint

The two key ideas in these analyses are that the Sun's rays are parallel to the Earth's surface at sunrise and sunset (therefore$\cos\alpha = 0$), and that at the instant of the March equinox, $\theta(t) - \theta_s = \pi/2$. Combining those two observations, we can deduce from Eq. (5.1) that at the instant of the March equinox sunrise, $\cos\lambda\sin k(\mu,t) = 0$. Thus, we have only two possibilities: either $\cos\lambda = 0$, or $\sin k(\mu,t) = 0$. The condition $\cos\lambda = 0$ would mean that at the instant of an equinox, sunset is occurring only at the north and south poles. We reject that possibility, because we know that sunsets are never experienced at only one single, precise latitude. Thus, we conclude that $\sin k(\mu,t) = 0$, and $\cos k(\mu,t) = \pm 1$.

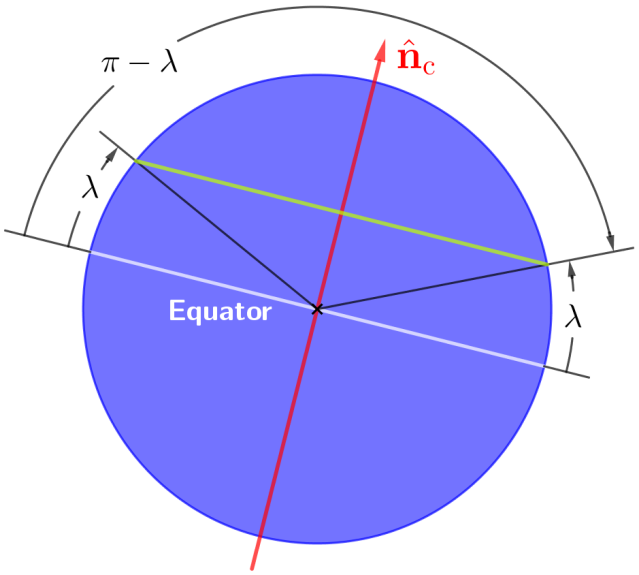

Figure 26: Because we measure latitudes from the equator, the latitudes λ and $\pi - \lambda$ are in fact the same latitude.

The azimuth at which the Sun rises and sets on the equinoxes Substituting $\sin k(\mu, t) = 0$ and $\theta(t) - \theta_s = \pi/2$ in Eq. (5.4), we find that the denominator of $\sin\beta$ is $\cos\lambda$. Next, substituting $\sin k(\mu, t) = 0$, $\theta(t) - \theta_s = \pi/2$, and $\cos k(\mu, t) = \pm 1$ in Eq. (5.2), the numerator of $\sin\beta$ is $\pm\cos\lambda$. Thus, $\sin\beta = \pm 1$.

What is the physical interpretation of that result? Let's go back and re-examine the condition $\sin k(\mu, t) = 0$. That condition is met by either of $k(\mu, t) = 0$ or $k(\mu, t) = \pi$. Recalling that $k(\mu, t) = \mu - \mu_s + \omega(t - t_s)$, we can now see that the condition $\sin k(\mu, t) = 0$ obtains at two longitudes: $\mu = \mu_s - \omega(t - t_s)$ and $\mu = \pi + [\mu_s - \omega(t - t_s)]$. The μ values of our two longitudes differ by π. One inference from that result is that the two longitudes are on opposite sides of the Earth. Another (from basic trig identities) is that signs of those longitudes' respective values of $\cos k(\mu, t)$ are opposite in algebraic sign. Therefore, of the two longitudes at which $\cos\alpha = 0$ at the instant of the March equinox, $\cos k(\mu, t)$ must be $+1$ for one of those longitudes, and -1 for the other.

Following through on that result, the numerators of $\sin\beta$for those longitudes are $+\cos\lambda$ and $-\cos\lambda$, respectively, making their respective values of $\sin\beta$ $+1$ and -1. Thus, one of those longitudes is experiencing sunrise, and the other is experiencing sunset.

The preceding analysis shows that for those two longitudes, $\cos\lambda \sin k(\mu, t) = 0$, regardless of latitude at the instant of the March equinox. That is, all latitudes are experiencing sunrise on one of those longitudes, and all latitudes are experiencing sunset on the other. Similar reasoning leads to the same conclusion for

the September equinox. This finding is familiar to anyone who drives eastward to work around daybreak on the equinoxes: the Sun will be almost directly in your eyes when on the drive to work in the morning, and again on the drive home just before sunset.

The longitude that experiences sunrise at the instant of an equinox, and the longitude that experiences sunset We'll use the March 2017 equinox as an example. We've seen (above) that $\sin k(\mu, t) = 0$. Because $k(\mu, t) = \mu - \mu_s + \omega(t - t_s) = \{\mu - [\omega(t - t_s) - \mu_s]\}$,

$$\sin\{\mu - [\omega(t - t_s) - \mu_s]\} = 0, \text{ giving}$$
$$\sin\mu\cos[\omega(t - t_s) - \mu_s] + \cos\mu\sin[\omega(t - t_s) - \mu_s] = 0.$$

That equation can be solved either algebraically or by inspection to find the sines and cosines of the longitudes μ_1 and μ_2 at which the Sun is either rising or setting:

1. $\sin\mu_1 = \sin[\omega(t - t_s) - \mu_s]$, $\cos\mu_1 = -\cos[\omega(t - t_s) - \mu_s]$;
2. $\sin\mu_2 = -\sin[\omega(t - t_s) - \mu_s]$, $\cos\mu_2 = \cos[\omega(t - t_s) - \mu_s]$.

For the March 2017 equinox, $t - t_s = 88.987$ days (Table 4). Using that value, plus $\omega = 6.00388$ radians/second (Table 3), we find that

1. $\sin\mu_1 = 0.909326$ and $\cos\mu_1 = -0.416084$; therefore $\mu_1 = 114.588°$, and ;
2. $\sin\mu_2 = -0.909326$ and $\cos\mu_2 = 0.416084$; therefore $\mu_2 = -65.412°$.

By comparison, Stellarium ([3]) shows the Sun setting at longitude 114.611° and rising at longitude −65.387° at the instant of the March equinox. Note that those values, like the ones calculated here, ignore the effects of atmospheric refraction upon the altitude of the Sun. For more about those effects, see [15].

Trajectory of the shadow's end point during the day of the March equinox From Fig. 27, the length, $\|\mathbf{s}(t)\|$, of the shadow cast by a gnomon of height $\|\mathbf{g}\|$ is $\|\mathbf{g}\|\tan\alpha(t)$. We wish to calculate the length of $\mathbf{s}(t)$'s projection upon the direction "local north". That length is $\|\mathbf{s}(t)\|\cos\beta(t)$.

As we've done in previous calculations for the March equinox, let's begin by finding $\cos\alpha(t)$ from Eq. (5.1). Because the quantity $\theta(t) - \theta_s$ differs little from $\pi/2$ throughout that day, we can take $\cos\alpha(t)$ as $\cos\alpha(t) = \cos\lambda\sin k(\mu, t)$. The denominator of $\cos\beta(t)$ (Eq. (5.3)) simplifies to

$$\textit{Denominator of } \cos\beta(t) = \cos\lambda\sqrt{1 - \left[-\underbrace{\cos\lambda\sin k(\mu, t)}_{=\cos\alpha(t)}\right]^2}$$
$$= \cos\lambda\sin\alpha(t).$$

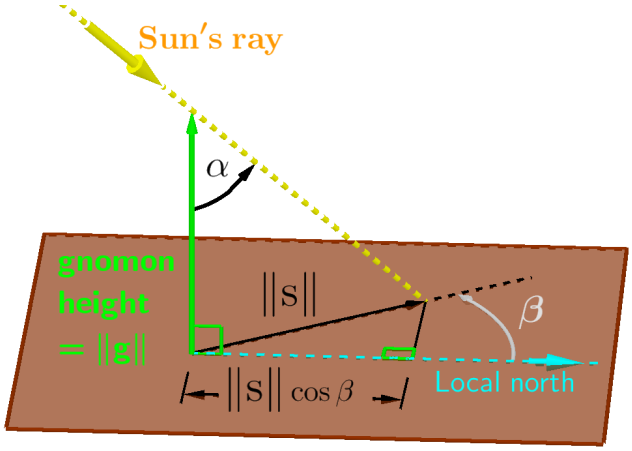

Figure 27: For simplicity, we've written the vector $\mathbf{s}(t)$ and the angles $\alpha(t)$ and $\beta(t)$ as $\mathbf{s}$, α, and β. The length, $\|\mathbf{s}\|$, of the shadow cast by a gnomon of height $\|g\|$ is $\|\mathbf{g}\| \tan\alpha$. We wish to calculate the length of $\mathbf{s}$'s projection upon the direction "local north" on the days of equinoxes.

From Eq. (5.3), the numerator of $\cos\beta(t)$ on the day of the March equinox can be taken as $\sin\lambda\cos\lambda\sin k(\mu,t)$, which is $\sin\lambda\cos\alpha(t)$. Therefore, $\cos\beta(t) = (\tan\lambda)/[\tan\alpha(t)]$. Assembling all of these ideas, the length of the projection of the shadow upon the direction "local north" is

$$\begin{aligned}\|\mathbf{s}(t)\|\cos\beta(t) &= [\|\mathbf{g}\|\tan\alpha(t)]\left[\frac{\tan\lambda}{\tan\alpha(t)}\right] \\ &= \|\mathbf{g}\|\tan\lambda.\end{aligned}$$

The interpretation of that result is that the trajectory of the end of the gnomon's shadow is a straight, east-west line at the distance $\|\mathbf{g}\|\tan\lambda$ from the base of the gnomon (Fig. 28). This striking phenomenon is one of the well-known behaviors of the gnomon's shadow (Section 2.1).

5.1.2 Azimuths of Sunrise and Sunset on the Solstices

We'll begin with the December solstice. As in the previous analysis, one of the key ideas is that $\cos\alpha = 0$ at sunrise and sunset. The other is that at the instant of the December solstice, $\theta(t) - \theta_s = 0$. Thus, Eq. (5.1) becomes

$$\cos(\eta+\lambda) - \cos\eta\cos\lambda(1-\cos k(\mu,t)) = 0. \tag{5.5}$$

Again because $\theta(t) - \theta_s$ varies little during the 24-hour period surrounding the instant of the December solstice, Eq. (5.5) should be very nearly true at sunset and sunrise for every point on Earth throughout that period. As a consequence of Eq. (5.5), and because $\theta(t) - \theta_s = 0$, the denominator of $\sin\beta(t)$

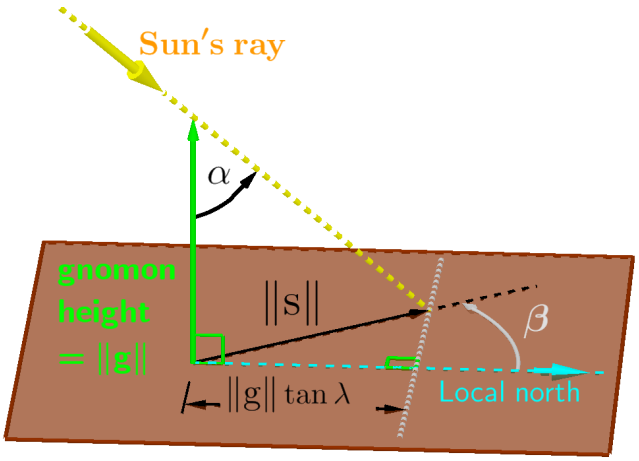

Figure 28: On the day of an equinox, the trajectory of the end of the gnomon's shadow is a straight, east-west line at the distance $\|\mathbf{g}\| \tan\lambda$ from the base of the gnomon.

and $\cos\beta\,(t)$ (see Eq. (5.4) and the discussion that precedes it) should differ only slightly from $\cos\lambda$ throughout the day of the December solstice.

A further consequence of Eq. (5.5) can be seen by using $\cos(\eta+\gamma) = \cos\eta\cos\gamma - \sin\eta\sin\gamma$, then rearranging to give

$$\cos\eta\cos\lambda\cos k\,(\mu,t) = \sin\eta\sin\lambda. \tag{5.6}$$

Using that result in Eq. (5.3), along with $\theta\,(t) - \theta_s = 0$, we obtain

$$\begin{aligned} \textit{Numerator of}\ \cos\beta\,(t) &= \cos\eta\cos\lambda\sin\lambda\cos k\,(\mu,t)\sin\eta\cos^2\lambda \\ &= [\cos\eta\cos\lambda\cos k\,(\mu,t)]\sin\lambda + \sin\eta\cos^2\lambda \\ &= [\sin\eta\sin\lambda]\sin\lambda + \sin\eta\cos^2\lambda \\ &= \sin\eta; \\ \therefore\ \cos\beta &= \frac{\sin\eta}{\cos\lambda}, \end{aligned} \tag{5.7}$$

because the denominator of $\cos\beta\,(t)$ is $\cos\lambda$.

Now, let's turn to $\sin\beta\,(t)$. Its numerator (Eq. (5.2)) reduces to

$$\textit{Numerator of}\ \sin\beta\,(t) = -\cos\eta\cos\lambda\sin k\,(\mu,t)\,.$$

We'll use Eq. 5.6 to develop an expression for $\sin k(t)$:

$$\begin{aligned} \cos\eta\cos\lambda\cos k\,(\mu,t) &= \sin\eta\sin\lambda; \\ \therefore\ \sin k\,(\mu,t) &= \pm\sqrt{1-\left(\frac{\sin\eta\sin\lambda}{\cos\eta\cos\lambda}\right)^2} \\ &= \pm\frac{\sqrt{\cos^2\eta\cos^s\lambda - \sin^2\eta\sin^2\lambda}}{\cos\eta\cos\lambda}. \end{aligned}$$

Making that substitution,

$$Numerator\ of\ \sin\beta\left(t\right) = \pm\sqrt{\cos^2\eta\cos^s\lambda - \sin^2\eta\sin^2\lambda};$$

$$\therefore\ \sin\beta\left(t\right) = \pm\frac{\sqrt{\cos^2\eta\cos^s\lambda - \sin^2\eta\sin^2\lambda}}{\cos\lambda}, \tag{5.8}$$

because the denominator of $\sin\beta\left(t\right)$ is $\cos\lambda$.

Confirm that $\sin\beta\left(t\right)$ and $\cos\beta\left(t\right)$, as given by the equations that we've developed here, do satisfy $\sin^2\beta\left(t\right) + \cos^2\beta\left(t\right) = 1$.

How do we interpret the expressions that we've derived for $\sin\beta\left(t\right)$ and $\cos\beta\left(t\right)$? Because Earth's η is positive, $\cos\beta\left(t\right)$ is positive, meaning that at sunset as well as at sunrise, the gnomon's shadow falls to the north of the point at which the gnomon is planted. We know that this prediction is correct, because the Sun rises and sets south of due east on the December solstice. Of $\sin\beta\left(t\right)$'s two values, the positive one is for sunrise (the shadow falls to the west of the gnomon because the Sun rises in the East), and the negative is for sunset.

In the case of San Cristóbal, $\lambda = 0.29211$ radians (Table 3), and $\eta = 0.40911$ radians. Using those values in Eqs. (5.7) and (5.8), $\sin\beta\left(t\right) = 0.90964$ and $\cos\beta\left(t\right) = 0.41539$. From the conversion formulas in Table 1, $\beta = 1.1424$ radians, or $65.46°$.

Stellarium ([3]) shows sunrise in San Cristóbal as occurring at UTC 12:38:53 on the day of the December 2016 solstice, at which time the Sun's azimuth is $114°32'25''$. The angle β between local north and the shadow cast by the gnomon would therefore be $65°27'35''$, which is equal to $65.46°$.

Similar analyses for the June solstice, when $\theta\left(t\right) - \theta_s = \pi$, give the same values of $\sin\beta$ as in Eq. (5.8), but $\cos\beta = -\frac{\sin\eta}{\cos\lambda}$.

What does the change in sign of $\cos\beta$ imply about the Sun's position on the horizon in each hemisphere on the dates of the solstices?

5.1.3 Solar Zeniths on the Solstices and Equinoxes

The key fact that we will use here is that for a Solar zenith, $\cos\alpha = 1$.

Latitudes at which zeniths occur on the solstices We'll consider the December solstice first. At that instant, $\theta\left(t\right) - \theta_s = 0$, so that Eq. (5.1) reduces to

$$\cos\left(\eta + \lambda\right) - \cos\eta\cos\lambda\left(1 - \cos k\left(\mu, t\right)\right) = 1.$$

We'll now make a brief aside to show that that condition can be met only if $\cos\left(\eta + \lambda\right) = 1$. In our model, η and λ are between $-\pi/2$ and $\pi/2$. Hence, the product $\cos\eta\cos\lambda$ cannot be negative. Nor can $1 - \cos k\left(\mu, t\right)$ be negative. Thus, the term $\cos\eta\cos\lambda\left(1 - \cos k\left(\mu, t\right)\right)$ cannot be negative. As a consequence, only if $\cos\left(\eta + \lambda\right) = 1$ can $\cos\left(\eta + \lambda\right) - \cos\eta\cos\lambda\left(1 - \cos k\left(\mu, t\right)\right)$ be equal to 1.

Therefore, $\lambda + \eta = 0$, and $\lambda = -\eta$. In other words, the Solar zenith on the December solstice occurs at the southern latitude that's equal to the Earth's inclination with respect to the Earth's orbit. That prediction is confirmed by the observation that on the date of the December solstice, the Solar zenith occurs on the Tropic of Capricorn.

A similar analysis for the June solstice, when $\theta(t) - \theta_s = \pi$, leads to $-\cos(\eta + \lambda) = 1$, and thus to $\lambda = \pi - \eta$. We've already seen that $\lambda = \eta$ and $\lambda = \pi - \eta$ are the same latitude (Fig. 26). Thus, our model predicts that the Solar zenith occurs at latitude η on the June solstice, a prediction confirmed by the fact that the zenith occurs on the Tropic of Cancer on that date.

Latitudes at which zeniths occur on the equinoxes For zeniths on the March equinox, when $\theta(t) - \theta_s = \pi/2$, Eq. (5.1) reduces to $\cos\lambda = 1$, meaning that $\lambda = 0$. That is, the zenith occurs on the equator, as is consistent with observations that the zeniths occur on the equator at the equinoxes. On the September equinox, when $\theta(t) - \theta_s = \pi/2$, Eq. (5.1) reduces to $-\cos\lambda = 1$; therefore, $\lambda = \pi$. However, that result, too, means that the zenith occurs on the equator (Fig. 26).

Longitudes at which solar zeniths occur on the solstices On the December solstices, $\theta(t) - \theta_s$ is a multiple of 2π. As noted above, Solar zeniths occur at times and places such that $\cos\alpha = 1$. Using this information, Eq. (5.1) becomes

$$\cos(\eta + \lambda) - \cos\eta\cos\lambda\left[1 - \cos k(\mu, t)\right] = 1.$$

Using the formula for the cosine of the sum of two angles, and then simplifying, we arrive at

$$-\sin\eta\sin\lambda + \cos\eta\cos\lambda\cos k(\mu, t) = 1.$$

In the process of identifying the latitude at which the Solar zenith occurs on the December solstice, we found that $\lambda = -\eta$. Therefore,

$$\sin^2\lambda + \cos^2\lambda\cos k(\mu, t) = 1,$$

giving $\cos k(\mu, t) = 1$. Because $k(\mu, t) = \mu - \mu_s + \omega(t - t_s) = \{\mu - [\omega(t - t_s) - \mu_s]\}$,

$$\cos\{\mu - [\omega(t - t_s) - \mu_s]\} = 1; \text{ thus}$$
$$\cos\mu\cos[\omega(t - t_s) - \mu_s] - \sin\mu\sin[\omega(t - t_s) - \mu_s] = 1.$$

By inspection, the solution to that equation is $\sin\mu = -\sin[\omega(t - t_s) - \mu_s]$, $\cos\mu = \cos[\omega(t - t_s) - \mu_s]$.

In the case of the December 2017 solstice (21/12/2017 16:28:00 UTC), $t - t_s = 365.239$ days. Using that value, plus other relevant data presented in Table 3, $\sin\mu = -0.923525$ and $\cos\mu = 0.383539$, which are the sine and cosine of $-67.447°$. By comparison, Stellarium shows that at that time, along latitude

S 23.44°, the Sun's maximum altitude was 89.995°, at longitude −67.419°. The very small difference between the altitude 89.995° and an exact Solar zenith is probably caused by rounding error in the given value of η and of the time of the December solstice.

On the June solstices, $\theta(t) - \theta_s$ is an odd-number multiple of π. Therefore, Eq. (5.1) becomes

$$\cos(\eta + \lambda) - \cos\eta \cos\lambda \left[1 - \cos k(\mu, t)\right] = -1.$$

In identifying the latitude at which the Solar zenith occurs on the June solstice, we found that $\lambda = \eta$. Therefore, using reasoning similar to that which we followed for the December solstices, we arrive at

$$\cos\{\mu - [\omega(t - t_s) - \mu_s]\} = 1, \text{ giving}$$
$$\cos\mu \cos[\omega(t - t_s) - \mu_s] - \sin\mu \sin[\omega(t - t_s) - \mu_s] = -1.$$

By inspection, the solution to that equation is $\sin\mu = \sin[\omega(t - t_s) - \mu_s]$, $\cos\mu = -\cos[\omega(t - t_s) - \mu_s]$.

In the case of the June 2017 solstice (21/06/2017 04:24:00 UTC), $t - t_s = 181.736$ days. Using that value, plus other relevant data presented in Table 3, $\sin\mu = 0.910524$ and $\cos\mu = -0.413457$, which are the sine and cosine of 114.422°. By comparison, Stellarium shows that at that time, along latitude N 23.44°, the Sun's maximum altitude was 89.994°, at longitude 114.450°. The very small difference between the altitude 89.994° and an exact Solar zenith is probably caused by rounding error in the given value of η and of the time of the June solstice.

5.2 Numerical Predictions of Sun's Azimuth and Elevation as Seen from Specific Locations at Specific Times

To obtain the values of $\theta(t)$ used in these predictions, I first employed Microsoft Excel's Solver tool to estimate $\phi(t)$ from Eq. (2.1)

$$\left[\frac{2\pi}{T}\right] t = \phi(t) - \epsilon \sin\phi(t),$$

then found $\theta(t)$ from Eq. (2.3):

$$\theta(t) = 2\tan^{-1}\left[\left(\frac{1+\epsilon}{1-\epsilon}\right)^{1/2} \tan\frac{\phi(t)}{2}\right].$$

Section 2.2.1 notes that the perihelion of 2017 occurred 12.93 days after the instant of the December 2016 solstice, at which time the angle θ was 0.2301 rad before perihelion. Thus, $\theta_s = -0.2301$ rad and $t_s = -12.93$ days.

Tables 5 and 6 compare calculated altitudes and azimuths to those obtained via Stellarium, for three different instants in Port Moresby and San Cristóbal de

Las Casas. Values of β were converted to azimuths as described in Table 1. For comparison, Table 7 shows the variation in the Sun's altitude and azimuth, as seen from San Cristóbal, at five-minute intervals around UTC 4 October 2071 22:30:00.

5.3 Discussion of Results from the Validations

Predictions derived from analyses of Eqs. (4.10), (4.11), (4.12), (4.13), and (4.14) are consistent with known characteristics of sunrises, sunsets, and Solar zeniths on solstices and equinoxes. Numerical predictions of longitudes at which those phenomena occur on said dates are within a few hundredths of a degree of Stellarium values.

The same is true for numerical calculations of the Sun's azimuths and altitudes as seen from Port Moresby and San Cristóbal de Las Casas. Except for the azimuths of the Sun at Solar zenith (an essentially meaningless quantity), all of the differences between calculated values and those obtained via Stellarium are much smaller than the Sun's changes in altitude and azimuth during five minutes. That result is perhaps surprising, because the need to estimate the timing of the "unperturbed" perihelion was, in itself, expected to cause errors equal to the Sun's changes in altitude and azimuth during five minutes ([7]).

6 Conclusions

The accuracy of our simple model's predictions should neither surprise us nor cause us to lose sight of our purpose. The predictions are accurate because the Earth is indeed nearly a perfect sphere, and because (as generations of experiments and observations confirm) its orbital parameters are as used herein. Our model's only real novelty—the use of an estimated "perturbed" perihelion—was known from [7] to be inaccurate by five minutes or less in timings of solstices and equinoxes; therefore, it should not have been expected to cause significant errors in our predictions.

Our real purpose, then, was to learn how we might express the Earth's movements conveniently in GA terms, after which we would learn how to manipulate the resulting expressions efficiently via GA to obtain equations that provide the answers that we needed. The route that we followed here was by no means the only one possible. For example, the draft version of this document used rotations of bivectors (as opposed to vectors) almost exclusively. I chose the result presented herein because it seemed to me to be the easiest to follow, and to implement in Maxima and Excel. Students and teachers experienced in using dedicated GA programs may see better ways of solving this problem. I will be grateful for their comments, criticisms, and suggestions, which I encourage them to post at the LinkedIn group "Pre-University Geometric

Table 5: Comparison of Sun's azimuths and altitudes according to atellarium, to Those calculated from Eqs. (4.10), (4.11), (4.12), (4.13), and (4.14), as seen from Port Moresby, Papua New Guinea on three dates in 2017. All of the calculations are implemented in [16].

UTC 24 February 2017 02:24:32 (Solar zenith)		
	Azimuth	Altitude
Calculated	289.16°	89.97°
From Stellarium	336.76°	89.99°
Calculated minus Stellarium	-47.60°	-0.02°
UTC 19 May 2017 03:00:00		
	Azimuth	Altitude
Calculated from	336.27°	58.05°
From Stellarium	336.30°	58.08°
Calculated minus Stellarium	-0.03°	-0.03°
UTC 15 October 2017 23:00:00		
	Azimuth	Altitude
Calculated	92.97°	46.38°
From Stellarium	92.97°	46.36°
Calculated minus Stellarium	0.00°	0.02°

Table 6: Comparison of Sun's azimuths and altitudes according to Stellarium, to those calculated from Eqs. (4.10), (4.11), (4.12), (4.13), and (4.14), as seen from San Cristóbal de Las Casas, Chiapas, Mexico on three dates in 2017. All of the calculations are implemented in [16].

UTC 6 May 2017 18:07:11 (Solar zenith)		
	Azimuth	Altitude
Calculated	278.94°	89.97°
From Stellarium	344.56°	90.00°
Calculated minus Stellarium	-65.62°	-0.03°
UTC 3 July 2017 18:00:00		
	Azimuth	Altitude
Calculated	28.87°	82.92°
From Stellarium	29.08°	82.92°
Calculated minus Stellarium	-0.21°	0.00°
UTC 4 October 2017 22:30:00		
	Azimuth	Altitude
Calculated	258.53°	19.74°
From Stellarium	258.52°	19.77°
Calculated minus Stellarium	0.01°	-0.03°

Table 7: Solar azimuths and altitudes as seen from San Cristóbal de Las Casas, according to Stellarium, at five-minute intervals around UTC 4 October 2071 22:30:00

	Time				
	22:20:00	22:25:00	22:30:00	22:35:00	22:40:00
Azimuth	257.61°	258.07°	258.52°	258.96°	259.39°
Altitude	22.11°	20.94°	19.77°	18.59°	17.42°

Algebra" (https://www.linkedin.com/groups/8278281).

References

[1] Eratosthenes Project, 2018, http://www.eratosthenes.eu/spip/IMG/jpg/2011-12-meerut_6_.jpg, accessed 30 March 2018.

[2] K. Krisciunas, (undated, untitled), http://people.physics.tamu.edu/krisciunas/gnomon.html, accessed 30 March 2018.

[3] Stellarium 0.15.1 Free Software Foundation, Inc. , 51 Franklin Street, Suite 500, Boston, MA 02110-1335, USA

[4] AstroPixels, undated, "Earth at Perihelion and Aphelion: 2001 to 2100", http://astropixels.com/ephemeris/perap2001.html, accessed 27 April 2017.

[5] NASA, 2016, "Earth Fact Sheet", https://nssdc.gsfc.nasa.gov/planetary/factsheet/earthfact.html, updated 23 December 2016, accessed 27 April 2017.

[6] D. Hestenes, 1999, *New Foundations for Classical Mechanics*, (Second Edition), Kluwer Academic Publishers (Dordrecht/Boston/London).

[7] J. A. Smith, 2017, "Estimation of the Earth's 'Unperturbed' Perihelion from Times of Solstices and Equinoxes", http://vixra.org/abs/1712.0642, 28 December 2017.

[8] Sidereal vs. Synodic Motions, http://astro.unl.edu/naap/motion3/sidereal_synodic.html. No date – accessed 13 March 2018.

[9] Sidereal, tropical, and anomalistic years, http://www.public.asu.edu/~mjwhite/Sidereal%20and%20tropical%20years.pdf. Undated, accessed 13 March 2018.

[10] Eratosthenes Project, undated, "The time the sun reaches its zenith for a given location", http://eratosthenes.ea.gr/Stellarium_Guidance.pdf, accessed 31 March 2018.

[11] J. A. Smith, "Formulas and Spreadsheets for Simple, Composite, and Complex Rotations of Vectors and Bivectors in Geometric (Clifford) Algebra", http://vixra.org/pdf/1712.0393v1.pdf, 11 December 2017.

[12] J. A. Smith, 2018, "Calculating the Angle Between Projections of Vectors Via Geometric (Clifford) Algebra", http://vixra.org/abs/1802.0047, 5 February 2018.

[13] A. Macdonald, *Linear and Geometric Algebra* (First Edition) p. 126, CreateSpace Independent Publishing Platform (Lexington, 2012).

[14] J. A. Smith, 2018, "Maxima Gnomon Formulas File for Publication (a Maxima file), https://drive.google.com/file/d/10X5AMSaVVVAEkW6uhxuvSr_7adnSWg1O/view?usp=sharing , 9 March 2017.

[15] Time and Date 2018, "What Is Refraction of Light?", https://www.timeanddate.com/astronomy/refraction.html, accessed 26 March 2018.

[16] J. A. Smith, 2018, "Spreadsheet for Gnomon Calculations and Sun's Azimuth and Elevation" (an Excel spreadsheet), https://drive.google.com/file/d/1W-T7hAdmyn7qLkUbqaUNN0eZ5Cp1qBFZ/view?usp=sharing, 9 March 2018.